Energy & Environmental Science

ROYAL SOCIETY OF CHEMISTRY

PAPER

View Article Online
View Journal | View Issue

Cite this: *Energy Environ. Sci.*, 2024, **17**, 3503

Global production potential of green methanol based on variable renewable electricity†

Mahdi Fasihi * and Christian Breyer

Methanol is a primary petrochemical globally. Green methanol, produced by Power-to-X technologies, is a potential solution to the defossilisation of the existing methanol supply and fossil fuel substitution. This study investigates the optimal system configuration for the lowest cost green e-methanol production from electrolytic hydrogen and atmospheric carbon dioxide based on an hourly power supply by hybrid PV-wind systems in a 0.45° × 0.45° spatial resolution. Results suggest that, by 2030, solar PV will be the dominating electricity generation technology in most parts of the world. For a weighted average cost of capital of 7%, e-methanol could be produced for a cost range of 1200–1500, 600–680, 390–430 and 315–350 € per t_{MeOH} (189–236, 94–104, 61–68 and 50–54 € per $MWh_{MeOH,HHV}$) at the best sites in 2020, 2030, 2040 and 2050, respectively. By 2040, the production cost of e-methanol will be within the market prices, suggesting that methanol supply could be defossilised at no extra cost for consumers. Conversely, e-methanol costs remain higher than the cost of natural gas-based methanol for fuel prices below 11 USD per MBtu. However, the introduction of up to 150 € per t_{CO_2} emissions cost could increase the cost of natural gas-based methanol to about 300 € per t_{MeOH} (47 € per $MWh_{MeOH,HHV}$), thus significantly improving the cost competitiveness of e-methanol in the market.

Received 4th September 2023,
Accepted 4th April 2024

DOI: 10.1039/d3ee02951d

rsc.li/ees

Broader context

The problem of global warming demands a massive reduction in anthropogenic greenhouse gas emissions, mainly carbon dioxide, by direct and indirect defossilisation of the entire energy-industry system. Green e-methanol could become a key platform chemical to defossilise most of the carbon-based feedstock in the chemical industry, and serve as a potential low-carbon fuel for long-range marine transportation. However, there is a knowledge gap in the global potential of low-cost e-methanol production in terms of scale. This paper evaluates the cost-volume potential of green e-methanol from 2020 to 2050, based on cost-optimised hybrid PV-wind power plants in high spatial resolution on a global scale. The results could be used in later research to identify the self-sufficient regions, as well as potential hubs for green e-methanol trading in a highly defossilised energy-industry system.

1. Introduction

Methanol (CH_3OH or MeOH) is the third major primary petrochemical globally.[1] The main derivatives of methanol include olefins, formaldehyde, acetic acid, methyl *tert*-butyl ether, methyl methacrylate and dimethyl ether that are used in automotive, construction, electronics, paints, pharmaceuticals and packaging.[2,3] Methanol is also partly used for gasoline blending or conversion to gasoline[4] as a transportation fuel.[3]

Global methanol production has experienced a steady growth over decades and reached 107 million tonnes per year, equal to 680 TWh_{MeOH} at higher heating value (HHV), in 2021.[5] Today, methanol is mainly produced from natural gas and partly from oil and coal, leading to a process emission of 0.5–1.5 tonne carbon dioxide (t_{CO_2}) per t_{MeOH} (79–236 kg_{CO_2} per $MWh_{MeOH,HHV}$).[6] Futhermore, with a carbon content of 0.375 t per t_{MeOH}, there is a potential for additional emissions of 1.375 t_{CO_2} per t_{MeOH} (216 kg_{CO_2} per $MWh_{MeOH,HHV}$) by incineration of methanol or its derivatives at the end of their lifespan. With respect to the urgency of climate change and in accordance with the Paris Agreement,[7,8] the mitigation of greenhouse gas (GHG) emissions from growing demand for methanol production is essential.

The production of methanol from sustainable and low-carbon feedstock and energy is an option to mitigate its GHG emissions. The declining cost of renewable electricity,

LUT University, Yliopistonkatu 34, 53850 Lappeenranta, Finland.
E-mail: mahdi.fasihi@lut.fi

† Electronic supplementary information (ESI) available. See DOI: https://doi.org/10.1039/d3ee02951d

especially solar photovoltaics (PV) and wind power,[9] together with advancements in industrial scale CO_2 direct air capture (DAC),[10] show potential to sustainably supply hydrogen by water electrolysis and CO_2 by DAC. Green methanol can then be produced directly from hydrogen and CO_2 in methanol synthesis plants, which are already deployed on a commercial scale.[11]

The compound annual growth rate of global methanol demand was 5.7% and 6.8% for the 2000–2021 and 2015–2021 periods, respectively.[3,5] For a compound annual growth rate of 5–7% with reference to the year 2021, the conventional demand for methanol in 2050 supplied by green methanol could reach 440–761 Mt per year (2799–4838 $TWh_{MeOH,HHV}$ per year), respectively. Green methanol can also substitute much of the remaining fossil fuels used in the chemical industry to produce other platform chemicals such as ethylene, propylene and BTX aromatics.[12,13] As such, the role of electricity-based green methanol in the chemical industry could drastically increase to up to 15 000–18 000 $TWh_{MeOH,LHV}$, depending on the share of biomethanol.[14] On the other hand, some platform or bulk chemicals could also be potentially produced directly from CO_2 and H_2 for a higher overall carbon and hydrogen conversion rate, which in return could reduce the overall demand for sustainable CO_2, green hydrogen, and green methanol in the chemical industry.[12] However, such technologies for direct conversion of CO_2 and H_2 to bulk chemicals are currently at a relatively lower technology readiness level[12] and their contribution to defossilisation of the chemical industry depends on their advancement in the coming decades. Green methanol is also a potential sustainable fuel for long-range marine transport.[15] Green methanol could also indirectly contribute to the transition to sustainable aviation fuel *via* the e-methanol-to-kerosene[16] route which has a higher carbon efficiency for CO_2-to-kerosene compared to power-to-kerosene *via* the Fischer–Tropsch process.[17] Such applications expand the demand for e-methanol beyond the chemical industry to the transportation industry. The technical feasibility of the power-to-methanol approach, together with the abundance of solar and wind resources, provide the potential to supply this elevated demand with renewable electricity-based methanol (e-methanol).

On a broader scale, the Methanol Economy[18,19] envisions a substitution of fossil fuels with methanol that overcomes the challenges of the earlier concept of the Hydrogen Economy.[20] While the Hydrogen Economy has regained interest in recent years,[21] both the Hydrogen Economy and the Methanol Economy may become a subset of the broader Power-to-X Economy[22] as power becomes the main primary energy carrier while hydrogen and methanol mainly act as intermediate energy and feedstock carriers. However, energy-industry system models are not yet prepared for an appropriate description of e-methanol and other e-fuels and e-chemicals.[23,24]

Traditionally, methanol has been produced from syngas (a mixture of carbon monoxide and hydrogen) from fossil fuels as the feedstock.[25] Syngas can also be produced from hydrogen and CO_2 *via* a reverse water–gas shift process.[26] However, starting from CO_2, methanol synthesis *via* direct CO_2 hydrogenation is preferred due to its higher energy and economic efficiency,[26] less cooling demand[27] and simpler plant design.[28]

The first commercial scale CO_2-to-methanol plant with 110 kt_{MeOH} per year capacity was commissioned by Carbon Recycling International (CRI) in China in 2022.[29] CRI's second methanol production facility from industrial waste CO_2 and H_2 with 100 kt_{MeOH} per year capacity is planned for commissioning in 2023 in China.[29] CRI is also designing the largest e-methanol plant in Europe with a 100 kt_{MeOH} per year capacity in Norway. The plant would use CO_2 from a ferrosilicon plant and hydrogen would be generated by water electrolysers powered by hydropower.[29]

The growing interest in low-carbon methanol has been reflected in academic literature in the past decade. Goeppert *et al.*[30] provided a comprehensive review on technologies for the conversion of CO_2 to methanol and its derivatives to close the loop of anthropogenic carbon in a Methanol Economy. Pérez-Fortes *et al.*[31] analysed a 440 kt per year methanol plant by the hydrogenation of CO_2 from a coal power plant. Michailos *et al.*[32] performed a techno-economic analysis and life cycle assessment on a 1 kt per day methanol plant based on captured CO_2 from flue gases and H_2 by proton exchange membrane (PEM) electrolysers. Hank *et al.*[33] performed an economic analysis of power-to-methanol in Germany *via* wind and grid power, PEM electrolysers and CO_2 from biogas and conventional ammonia plants. Dieterich *et al.*[27] provided an overview of the state-of-the-art synthesis technologies and pilot plants for methanol, DME and Fischer–Tropsch fuels. Abad *et al.*[34] simulated a lab-scale power-to-methanol system with integrated solid oxide electrolysis for hydrogen production and use of a side O_2 stream for partial oxy-combustion and CO_2 capture for methanol synthesis. Nizami *et al.*[35] performed a techno-economic and environmental assessment on power-to-methanol by PV-battery and PV-grid as power options, PEM electrolyser and CO_2 from natural gas field processing. The cost of power-to-methanol-to-gasoline/diesel based on a PV-battery power system and high temperature liquid solvent DAC in Saudi Arabia was studied by Ravi *et al.*[36] Bellotti *et al.*[37] and Atsonios *et al.*[38] studied the feasibility of methanol production by CO_2 captured from fossil power plants and the use of excess electricity from the grid for hydrogen generation by water electrolyser. Palys and Daoutidis[39] reviewed both production and utilisation technologies for e-methanol, as well as e-hydrogen and e-ammonia. Bos *et al.*[40] evaluated the cost of e-methanol production *via* a 100 MW power-to-methanol system based on a wind power plant, electrolyers and CO_2 direct air capture. Svitnič and Sundmacher[41] assessed the optimised system configuration and the cost of relatively small-scale power-to-methanol systems (40 kt_{MeOH} per year) *via* a range of power and heat generation and balancing technologies, PEM and solid oxide water electrolysers, and solid sorbent CO_2 direct air capture in 2019 and 2030 at Port Arthur, Texas, USA.

As can be seen, the literature on CO_2-to-methanol is mainly focused on case studies at locations with access to point source CO_2. Some of these sources, such as CO_2 from coal power plants, are unsustainable and likely not available in the long term as a steady source of CO_2. Only sustainable or unavoidable sources of CO_2, such as pulp and paper mills, waste incinerators, and cement mills would be relevant for CO_2-to-X applications. While less costly than atmospheric CO_2, global supply of CO_2 from point sources is significantly lower than the long-term demand for CO_2-to-X applications.[23] It could also face the challenge of colocation with the source of low-cost renewable electricity for the generation of low-cost hydrogen. Nevertheless, wherever possible, the benefits of co-location of point sources of CO_2 could reduce the cost of CO_2-to-X chains and help CO_2-to-X products ramp up production capacity, while DAC matures and its economics improve, becoming a long-term supplier of sustainable CO_2. To truly evaluate the potential of point sources of CO_2 for CO_2-to-X applications, their cost-volume data in high spatial resolution, together with possible routes and means of CO_2 transportation are required, which are beyond the scope of this study.

In this study, we investigate the cost and generation potential of e-methanol by hourly optimised atmospheric CO_2 capture and hydrogenation *via* hybrid PV-wind power-to-methanol systems with $0.45^\circ \times 0.45^\circ$ spatial resolution on a global scale from 2020 to 2050. We also report on the technology mix required to achieve the least cost fuel production and operational behaviour. To our knowledge, this is the first study with hourly optimisation of power-to-methanol systems in a high spatial resolution on a global scale.

To put the findings into perspective, a cost comparison of e-methanol and conventional methanol production is provided. In addition, the energetic cost comparison of e-methanol and e-ammonia[42,43] as potential sustainable fuels for the long-range marine sector,[15] as well as potential benefits of power-to-ammonia/methanol system integration are briefly discussed in the Results and discussion section.

2. Methods and data

2.1. Description of flexible onsite hybrid PV-wind power-to-methanol supply chain

The considered power-to-methanol chain is illustrated in Fig. 1, where all units are located at the same site (Onsite Scenario). The production chain includes three sources of power (fixed tilted PV, single-axis tracking PV and wind power plants). The generated power could be balanced prior to consumption through independently scalable battery storage and battery interface, with excess electricity being curtailed. Hydrogen-fuelled open cycle (H_2-OCGT) and combined cycle gas turbines (H_2-CCGT) are also included as potential seasonal power balancing solutions from 2030 onwards.[44] A cluster of alkaline water electrolysers uses electricity to convert water to hydrogen and oxygen at 30 bar. Oxygen is vented to the air while hydrogen

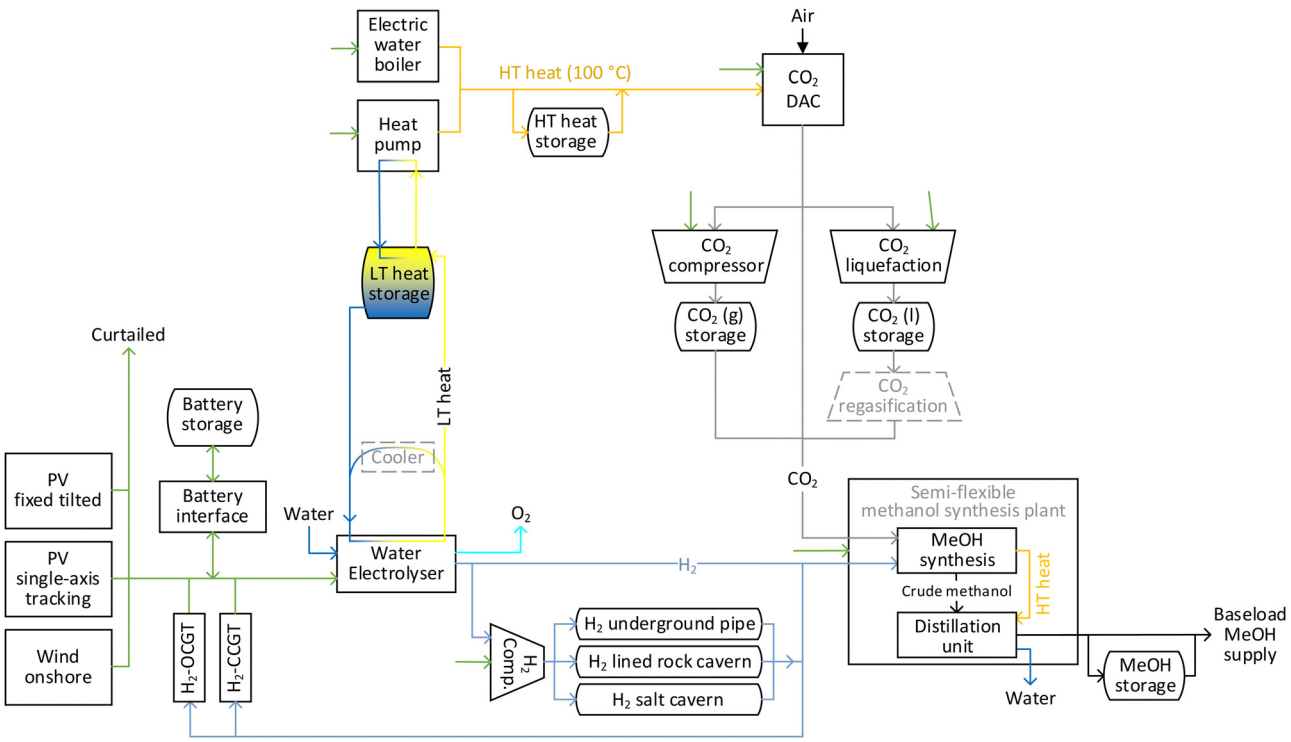

Fig. 1 Power-to-methanol Onsite model configuration. Hydrogen-fuelled gas turbines are considered from 2030 onwards. Abbreviations: H_2-fuelled open cycle gas turbine (H_2-OCGT), H_2-fueled combined cycle gas turbine (H_2-CCGT), compressor (Comp.), high temperature heat (HT heat), low temperature heat (LT heat), CO_2 direct air capture (DAC), and direct electric heater (DEH).

is fed to the semi-flexible methanol synthesis plant. While a single alkaline electrolyser stack has a limited minimum operational load, with load management, a cluster of stacks can provide a full range operational capacity by running only one stack at its minimum load. The hydrogen flow to the methanol synthesis unit could be balanced *via* intermediate storage options,[45,46] namely salt cavern, lined rock cavern and underground pipes. The construction of salt and rock cavern hydrogen storage options is limited to the regions with appropriate geological formations, whereas no restrictions are considered for the construction of an underground pipe system. The maximum pressure at hydrogen storage units is 150 bar, which is provided by multi-stage compressors. The maximum hourly charge and discharge rate of each storage option are limited (values in Table S8, ESI†) for temperature regulation of the storage and to avoid extra tension on salt cavern walls. CO_2 is captured at 1 bar by low temperature CO_2 DAC units. The captured CO_2 is then guided to the methanol synthesis unit. Prior to consumption, the CO_2 flow could be balanced *via* a CO_2 compression and storage system, as well as a CO_2 liquefaction and storage system. For the latter system, a regasification unit is required before supplying the CO_2 to the synthesis unit, which is not modelled separately in this study considering the abundance of low temperature waste heat in the system. The considered low temperature solid sorbent DAC technology requires heat at 100 °C in the form of water or steam for CO_2 regeneration.[47] The heat could be supplied by electric water boilers and heat pumps. The waste heat from electrolysers at 75 °C is stored in the form of warm water, which is then used as the heat source for the heat pumps. The 100 °C water flow could be balanced by intermediate storage in a hot water tank prior to utilisation in the DAC units. The hot water used at DAC units for CO_2 regeneration is assumed to be recycled at 78 °C and recirculated to the heat pump and electric boiler.

The technical assumptions of methanol synthesis plants for the direct conversion of CO_2 and hydrogen to methanol are based on the model by Pérez-Fortes *et al.*[31] The methanol synthesis reactor operates at 210 °C and 76 bar and has a carbon conversion rate of 22% per path. Accordingly, the package includes compressors for elevating the pressure of newly fed and recycled gases to the reactor pressure. The plant's overall carbon conversion rate is 94%, which is in line with 94.5% conversion ratio of the Shunli CO_2-to-Methanol Plant by CRI in China.[11] The methanol synthesis is exothermic and produces water as by-product. The excess heat is partly used by a distillation subunit for separation of water from methanol, making the overall methanol plant heat neutral. The plant requires external power to run the compressors and the rest of the facilities. The economic assumptions for the methanol synthesis plant are based on the reported cost for CRI's 110 kt per year CO_2-to-methanol plant, to which the cost of methanol storage is added for one month of storage as a safety measure. Today, conventional methanol plants could be designed for capacities up to 10 000 tonne per day ($\sim$3.3 Mt_{MeOH} per year). The benchmark capacity of the theoretical e-methanol plant in 2020 is assumed to be 0.5 Mt_{MeOH} per year, which gradually increases to 1, 2 and 3 Mt_{MeOH} per year in 2030, 2040 and 2050, respectively, to account for an increase in global demand for e-methanol. The cost of the methanol plant at each benchmark capacity is calculated based on a scaling factor of 0.78[48] applied on the cost of the 110 kt per year plant. In a conservative approach, the capex reduction from 2020 to 2050 is solely based on economies of scale and no learning rate is considered for further capex reduction by mass deployment. The methanol plant is semi-flexible with a minimum operational load of 50% and hourly ramp up/down of 2%/20%. A baseload supply of e-methanol is modelled, thus additional methanol storage is considered to balance methanol flows.

2.2. Hourly model and optimisation

All components and their hourly energy and mass balance are modelled in Matlab version R2020a[49] as shown in eqn (1) and the battery losses and state of charge are formulated in eqn (2). Abbreviations: flow type (f), hour (h), technology (t), generation (Gen), consumption (Con), charge (char), discharge (disc), state of charge (SoC), and storage for flow type (fs).

The relevant technologies to each flow type are as follows:

$\forall h \in [1, 8760] | \forall f \in [el, H_2, CO_2, LTH, HTH, MeOH]$:

$$\sum_{t}^{tech} \mathrm{Gen}_{f,h,t} - \sum_{t}^{tech} \mathrm{Cons}_{f,h,t} - \sum_{t}^{tech} \mathrm{storage\,char}_{f,h,t} + \sum_{t}^{tech} \mathrm{storage\,disc}_{f,h,t} + \sum_{t}^{tech} \mathrm{storage\,loss}_{f,h,t} - \sum_{t}^{tech} \mathrm{excess}_{f,h,t} = \sum_{t}^{tech} \mathrm{target\,demand}_{f,h,t} \quad (1)$$

constraints: $[\mathrm{Gen}_{f,h,t} | \mathrm{Cons}_{f,h,t} | \mathrm{storage\ char}_{f,h,t} | \mathrm{storage\ disc}_{f,h,t} | \mathrm{storage\ loss}_{f,h,t} | \mathrm{excess}_{f,h,t} | \mathrm{target\ demand}_{f,h,t}] \geq 0$

$\forall h \in [1, 8760] | \forall fs \in [el, H_2, CO_2, LTH, HTH, MeOH\ storage]$:

$$\mathrm{SoC}_{fs,h} = \mathrm{SoC}_{fs,h-1} \cdot (1 - \mathrm{self\ disc\ \ eff.}_{fs}) - \frac{\mathrm{disc}_{fs,h}}{\mathrm{disc\ \ eff.}_{fs}} + \mathrm{char}_{fs.h} \cdot \mathrm{char\ eff.}_{fs}$$
$$\mathrm{SoC}_{fs,1} = \mathrm{SoC}_{fs,8760} \cdot (1 - \mathrm{self\ disc\ \ eff.}_{fs}) - \frac{\mathrm{disc}_{fs,1}}{\mathrm{disc\ \ eff.}_{fs}} + \mathrm{char}_{fs,1} \cdot \mathrm{char\ eff.}_{fs} \quad (2)$$

• Tech f(el) {fixed tilted PV power plant, single-axis tracking PV power plant, wind power plant, H_2-fuelled open cycle gas turbine, H_2-fuelled combined cycle gas turbine, battery interface, battery storage, water electrolyser, methanol plant, H_2 compressor, DAC, CO_2 compressor, CO_2 liquefaction unit, heat pump, electric water boiler}

• Tech f(H_2) {water electrolyser, methanol plant, H_2 compressor, H_2 salt cavern, H_2 rock cavern, H_2 underground pipe, H_2-fuelled open cycle gas turbine, H_2-fuelled combined cycle gas turbine}

• Tech f(CO_2) {DAC, methanol plant, CO_2 compressor, CO_2 liquefaction unit, CO_2(g) storage, CO_2(l) storage}

• Tech f(LTH) {water electrolyser, LTH storage, heat pump}

• Tech f(HTH) {DAC, heat pump, electric water boiler, HTH storage}

• Tech f(MeOH) {methanol plant, MeOH storage, MeOH supply}

The levelised cost of methanol is calculated based on the NREL guideline,[50] as shown in eqn (3a)–(3c). Abbreviations: annuity factor (crf), weighted average cost of capital (WACC), lifetime, (N), applied technology (i), capital expenditures per unit of capacity (Capex), annual operational expenditures per unit of capacity (Opex), installed capacity (instCap), and annual generation (Gen).

$$\text{Levelised cost of methanol} = \frac{\sum_{i}^{\text{tech}} \left(\left(\text{Capex}_i \cdot \text{crf}_i + \text{Opex}_{\text{fix},i} \right) \cdot \text{instCap}_i + \text{Opex}_{\text{var},i} \cdot \text{Gen}_i \right)}{\text{Annual methanol supply}} \tag{3a}$$

$$\text{crf} = \frac{\text{WACC} \cdot (1+\text{WACC})^{\text{N}}}{(1+\text{WACC})^{\text{N}} - 1} \tag{3b}$$

$$\text{Gen}_i = \sum_{h=1}^{8760} \text{Gen}_{i,h} \tag{3c}$$

$$\text{Non-negativity constraints: } \left[\text{instCap}_i | \text{Gen}_{i,h} \right] \geq 0$$

A global uniform real WACC of 7% is used in all the calculations, excluding the inflation rate considered in nominal WACC. Assuming an equity share of 30% and an interest rate of 4%, a WACC of 7% would lead to a return on equity of 14%. Interest rates have been more uncertain in the past two years (2022–2023) due to measures taken by central banks to combat inflation. WACC of 7% represents the long-term WACC and the impact of actual WACC deviation by time and place has been addressed *via* sensitivity analysis of e-methanol production for a WACC of 5–9%.

To achieve the lowest production cost, a commercial linear optimiser, Mosek,[51] with continuous variables is used to find the ideal mix of installed capacities and hourly flows to minimise the annualised cost of the system for a small-size hourly (Gen_h = 1000 kg h^{-1}), and consequently annual (Gen = 8760 t per year), supply of e-methanol within the system constraints (eqn (4a)–(4f)).

$$\min \left(\sum_{i}^{\text{tech}} \left(\left(\text{Capex}_i \cdot \text{crf}_i + \text{Opex}_{\text{fix},i} \right) \cdot \text{instCap}_i + \text{Opex}_{\text{var},i} \cdot \text{Gen}_i \right) \right) \tag{4a}$$

$$\text{instCap}_i \geq \frac{\text{maximum hourly flow}_i}{\text{availability}_i} \tag{4b}$$

$$\text{instCap}_i \geq \frac{\text{maximum hourly SoC}_i}{\text{availability}_i} \tag{4c}$$

$$\text{Minimum operational load: } \text{Gen}_{i,h} \geq \text{instCap}_i \cdot \text{availability}_i \cdot \text{minimum load}_i \tag{4d}$$

$$\text{Ramp-up limit: } (\text{Gen}_{i,h} - \text{Gen}_{i,h-1}) \leq \text{instCap}_i \cdot \text{rampup rate}_i \cdot \text{availability}_i \tag{4e}$$

$$\text{Ramp-down limit: } (\text{Gen}_{i,h-1} - \text{Gen}_{i,h}) \leq \text{instCap}_i \cdot \text{ramp down rate}_i \cdot \text{availability}_i \tag{4f}$$

The hourly optimisations are executed independently for each year in a 0.45° × 0.45° spatial resolution based on hourly solar and wind potentials, as well as suitable geological formations[52] for hydrogen storage at the same node, shortly referred to as Onsite Scenario.

The hourly feed-in data of fixed-tilted PV is based on Gerlach *et al.*[53] and Huld *et al.*,[54] and the feed-in time series of single-axis tracking PV are based on Afanasyeva *et al.*[55] The hourly feed-in time series of wind turbines are according to Gerlach *et al.*,[53] which considers ENERCON standard 3 MW wind turbines (E-101) with 150-meter hub height. A wake effect of 8% is considered on the overall electricity generation of wind farms.

2.3. Theoretical production potential of e-methanol

Open seas, lakes and Antarctica have been excluded from the simulations. For the rest of the world, the area available for installation of solar PV and wind power plants each has been limited to 10% of each 0.45° × 0.45° nodal area to roughly account for other limitations for locations with technical potential for the installation of Power-to-X systems. A fixed global average installation density of 8.4 MW km^{-2} is assumed for a wind power installation from 2020 to 2050,[56] as the installation density of wind power plants has not improved over the past decade. The average solar PV installation density of fixed tilted and single-axis tracking PV follows the trend of the past decades and improves over time as specified in Table S8 (ESI†). A relatively small optimisation sample (1000 kg_{MeOH} hourly baseload supply and consequently 8760 t_{MeOH} annual supply (Gen)) is chosen to ensure that PV and wind installed capacities would be within their area limit. The optimal configuration of the nodal power-to-methanol system and consequently its methanol production could then be expanded to the point that either PV or wind installation reaches its area limit, as formulated in eqn (5a)–(5f). The global e-methanol production potential is the cumulative nodal e-methanol potential, as shown in eqn (5g).

PV (optimised hybrid fixed tilted-single axis tracking) installation density (instDens)

$$= \frac{\text{instDens}_{\text{fixed tilted}}\ [\text{MW km}^{-2}] \cdot \text{instCap}_{\text{fixed tilted}}\ [\text{MW}] + \text{instDens}_{\text{single-axis}}\ [\text{MW km}^{-2}] \cdot \text{instCap}_{\text{single-axis}}\ [\text{MW}]}{\text{instCap}_{\text{fixed tilted}}\ [\text{MW}] + \text{instCap}_{\text{single-axis}}\ [\text{MW}]} \quad (5a)$$

$$\text{Nodal area}\ [\text{km}^2] = \left(\frac{\text{polar circumference}\ [\text{km}]}{2} \cdot \frac{0.45^\circ}{180^\circ}\right)\left(\text{equatorial circumference}\ [\text{km}] \cdot \frac{0.45^\circ}{360^\circ} \cdot \text{Cosine}(\text{latitude}^\circ)\right) \quad (5b)$$

$$\text{PV multiplication factor} = \frac{\text{PV installation density}\ [\text{MW km}^{-2}] \cdot \text{nodal area}\ [\text{km}^2] \cdot 10\%\ \text{area limit}}{\text{instCap}_{\text{fixed tilted PV}}\ [\text{MW}] + \text{instCap}_{\text{single-axis PV}}\ [\text{MW}]} \quad (5c)$$

$$\text{Wind multiplication factor} = \frac{\text{wind installation density}\ [\text{MW km}^{-2}] \cdot \text{nodal area}\ [\text{km}^2] \cdot 10\%\ \text{area limit}}{\text{instCap}_{\text{wind}}\ [\text{MW}]} \quad (5d)$$

$$\text{Minimum multiplier} = \text{Min}(\text{PV multiplication factor, wind multiplication factor}) \quad (5e)$$

$$\text{Nodal production potential} = \text{minimum multiplier}_n \cdot \text{Gen}_n \quad (5f)$$

$$\text{Global production potential} = \sum_n^{\text{node}} \text{minimum multiplier}_n \cdot \text{Gen}_n \quad (5g)$$

As the nodal area differs by latitude, the e-methanol production potential per km^2 at each node is introduced (eqn (6)) for a better comparison of regional methanol production potentials.

$$\text{Regional production potential per km}^2 = \frac{\text{Nodal production potential}}{\text{nodal area}} \quad (6)$$

3. Results and discussion

3.1. Technology mix and levelised cost of electricity

Low-cost electricity with sufficient availability is a pilar of low-cost Power-to-X products. The global maps for Full Load hours (FLh) and levelised cost of electricity generation by fixed tilted and single-axis tracking PV, as well as wind power plants in 2020–2050 are provided in Fig. S1–S3 (ESI†). The hourly optimisation results in Fig. 2 show that, by 2030, PV is the dominating source of electricity generation for e-methanol production in most parts of the globe apart from Patagonia, Central and Northern Europe, the Midwestern US, and most regions at latitude above 60°N. By 2050, PV-dominated regions expand around the globe, particularly in Patagonia and Central Europe and the US. A comparison to the available literature shows that Svitnič and Sundmacher[41] also found a PV-dominated system lower in cost than a wind-based one at Port Arthur, Texas, USA in 2020 (Fig. S4, ESI†).

About 2–10% of the generated electricity by the cost-optimised hybrid PV-wind system is curtailed in most parts of the world in 2030. However, up to 40% curtailment is observed in Eastern Russia as a balancing solution due to a very high seasonality of power. As electricity generation gets cheaper by 2050, the curtailment rates generally increase 2–10 percentage points around the globe. Decker *et al.*[57] and Svitnič and Sundmacher[41] also found curtailment as part of the cost-optimised solution.

The role of batteries in supplying electricity to the final use is up to 5% of the total electricity demand in 2030 and 2050, as batteries are mainly used as a short-term power balancing solution to supply electricity to demands with a high utilisation rate such as electricity used by DAC units, heat pump and the methanol synthesis plant. A direct correlation is observed among regions with high shares of PV and regions with high shares of battery. No balancing role is observed for hydrogen-fuelled gas turbines. While not fully comparable, Nizami *et al.*[35] also reported about 60% higher e-methanol production costs (1670 USD per t) for a baseload PV-battery system, compared to a baseload PV-grid system in Indonesia.

While the levelised cost of electricity generation by hybrid PV-wind plants is only based on their technology mix, the cost of delivered electricity to the final user is affected by the additional cost of balancing solutions, namely curtailment, battery, and H_2-fuelled gas turbines. As illustrated in Fig. 3, while the levelised cost of electricity generation at the best sites declines from 20–25 € per MWh in 2020 to 7–10 € per MWh in 2050, the cost of delivered electricity to the final use declines from 25–30 € per MWh to 8–11 € per MWh, respectively.

3.2. Levelised cost and production potential of e-methanol

The results, as illustrated in Fig. 4, show that e-methanol could had been produced in 2020 for a cost range of 1200–1500 € per t_{MeOH} (189–236 € per $MWh_{MeOH,HHV}$) at the best sites in the world, such as Patagonia, the Atacama Desert, Tibet, the Horn of Africa, the Midwestern US, parts of Northern Africa and theoretically most of Greenland with technical potential in coastal regions. In 2020, apart from the Atacama Desert, the energy mix for the rest of the best sites is dominated by wind power. By 2030, the production cost of e-methanol at the best sites could decline to 600–680 € per t_{MeOH} (94–107 € per $MWh_{MeOH,HHV}$) in all continents with PV-dominated sites becoming the majority. By 2040, the PV-dominated regions

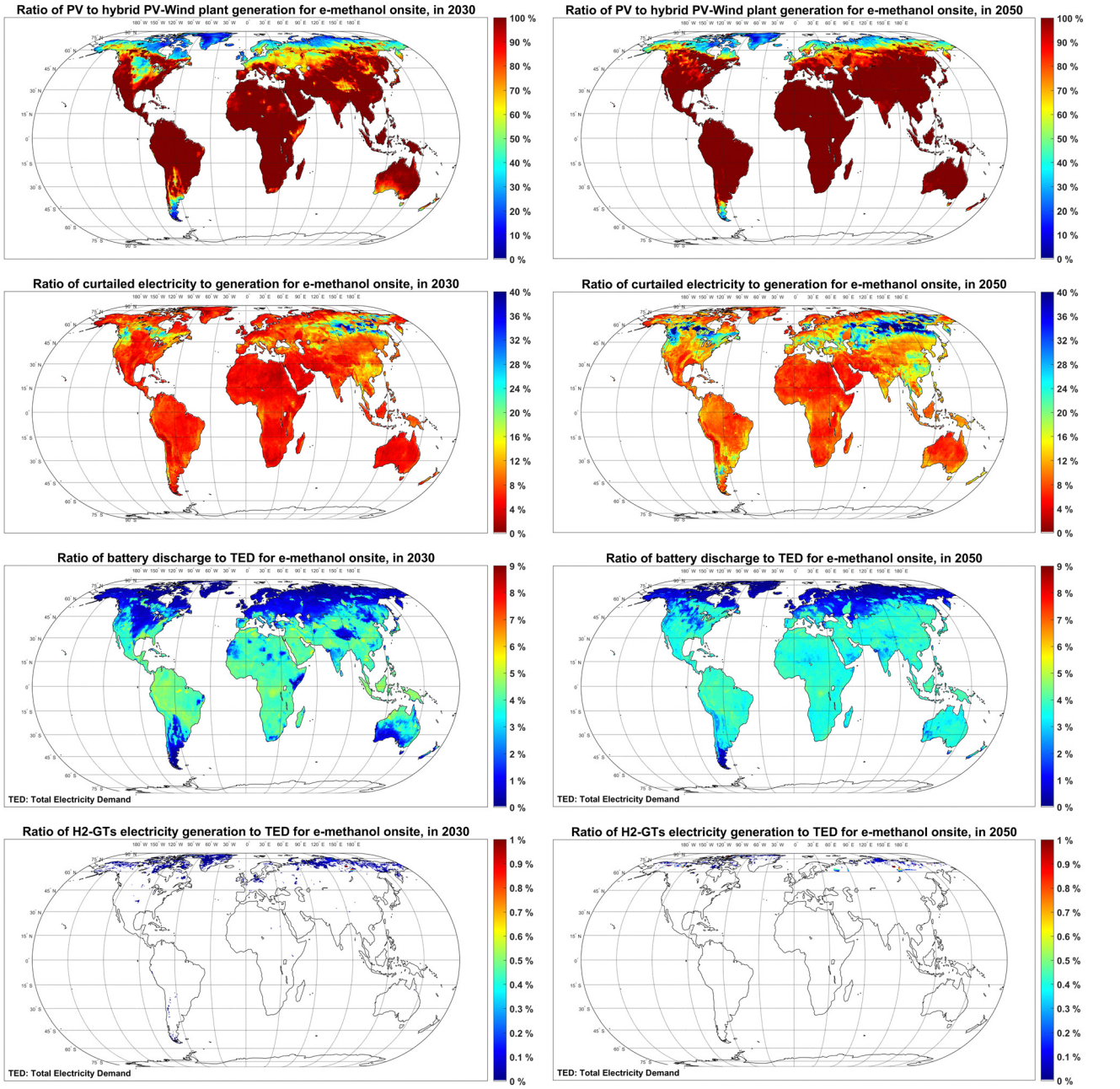

Fig. 2 Ratio of PV to hybrid PV-wind installed capacity (top), ratio of curtailed electricity (upper centre), ratio of battery discharge to total electricity demand (TED) (lower centre), and ratio of hydrogen-fuelled gas turbines (CCGT and OCGT) generation to TED for e-methanol Onsite (bottom) in 2030 (left) and 2050 (right).

take the lead at producing the least cost e-methanol at 390–430 € per t_{MeOH} (61–68 € per $MWh_{MeOH,HHV}$), which is bluntly visible for a comparison between Atacama Desert and Patagonia. The relatively sharper cost reduction of e-methanol at PV-dominated regions is due to a combination of factors. Firstly, a sharper capex decline projected for PV compared to wind power provides relatively lower cost PV electricity. Secondly, as the capex of electrolyser plants declines, running electrolysers at lower utilisation rates becomes economically more viable. Thirdly, the close-to-baseload electricity demand by the DAC plant and its heat suppliers significantly declines from 2020 to 2050, which makes providing electricity *via* PV and, by then cheaper batteries, less impactful on the total production cost of e-methanol. By 2050, e-methanol could be produced for 315–370 € per t_{MeOH} (50–58 € per $MWh_{MeOH,HHV}$) widely in all continents, and Atacama Desert remains the lowest cost region. Nevertheless, the large demand for sustainable methanol and relatively higher production costs and area limit in Europe, as well as the relatively low cost of methanol shipping may lead to global trading of e-methanol at a large scale.[24]

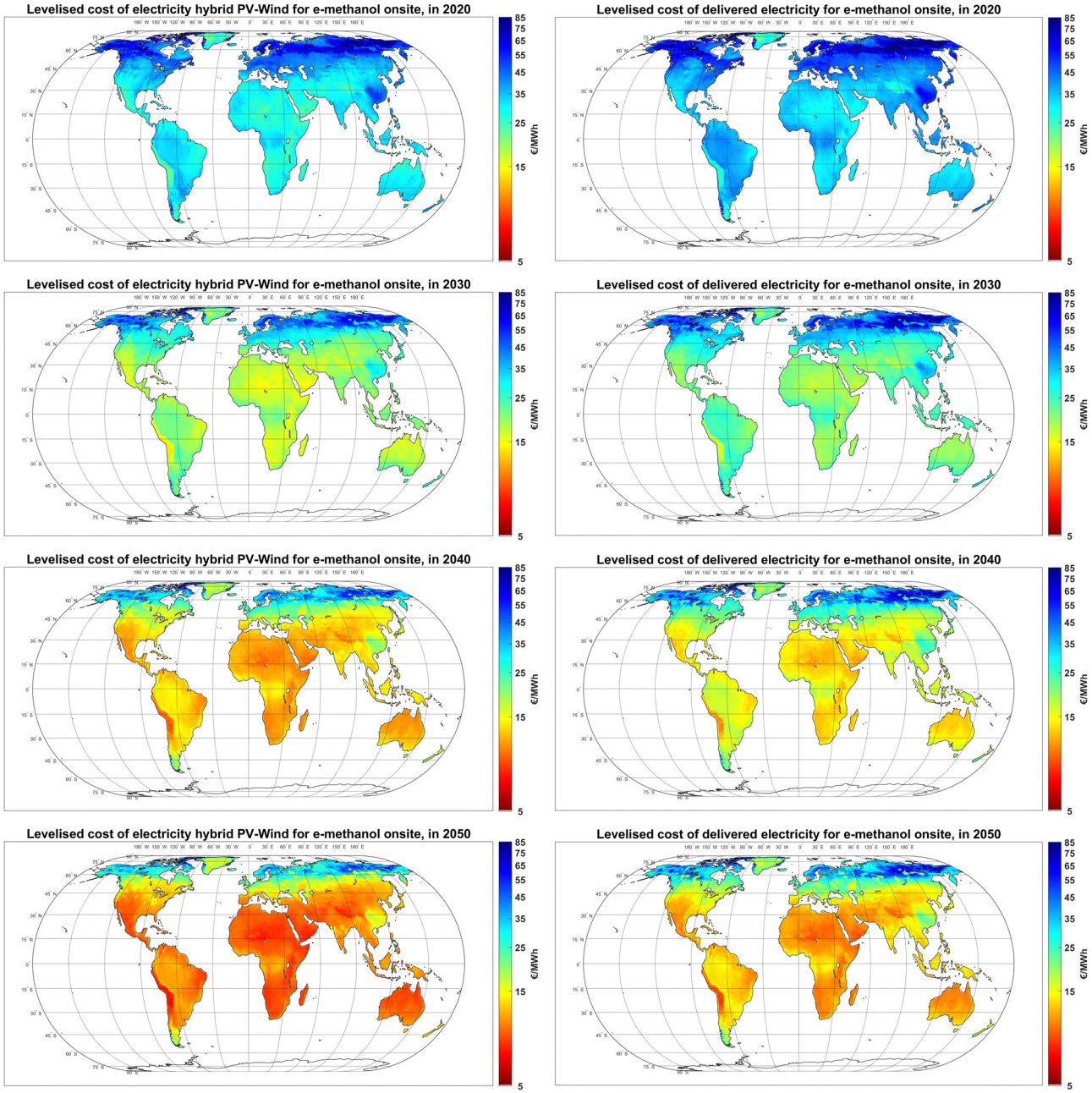

Fig. 3 Levelised cost of hybrid PV-wind electricity generation (left) and levelised cost of delivered electricity to final use (right) for 2020 (top), 2030 (upper centre), 2040 (lower centre) and 2050 (bottom).

Although different in assumptions, the results are comparable with the literature on case studies of e-methanol production. Bos *et al.*[40] reported on a cost range of 750–800 € per t_{MeOH} from atmospheric CO_2 and wind power in the Netherlands in the near future, which is slightly lower than our results for the same region in 2030.

Of the studies based on point sources of CO_2, Atsonios *et al.*[38] reported on e-methanol production costs of 800–1700 € per t for CO_2 from a coal power plant, an electricity price range of 20–60 € per MWh, and a 0.25–0.5 availability factor, comparable to our results in 2030. Svitnič and Sundmacher[41] reported on a minimum production cost of 1392 and 799 USD per t_{MeOH} at Port Arthur, Texas, USA, in 2019 and 2030, respectively. In our study, the cost of e-methanol production in the same region in 2020 and 2030 is 1600 and 700 € per t_{MeOH}, respectively. The relatively large difference in 2019–2020 cost estimations between the two studies is mainly due to about 3 times higher cost of DAC in our study. Chen and Yang.[58] reported on 787–1496 and 777–1852 USD per t e-methanol production from point source CO_2 and H_2 from electrolysis *via* flexible methanol plants in Norderney, Germany (wind-based) and Kramer Junction, US (solar PV-based), respectively. The lower and upper end of the given cost ranges represent a progressive and a conservative scenario, respectively. Their conservative results for e-methanol based on

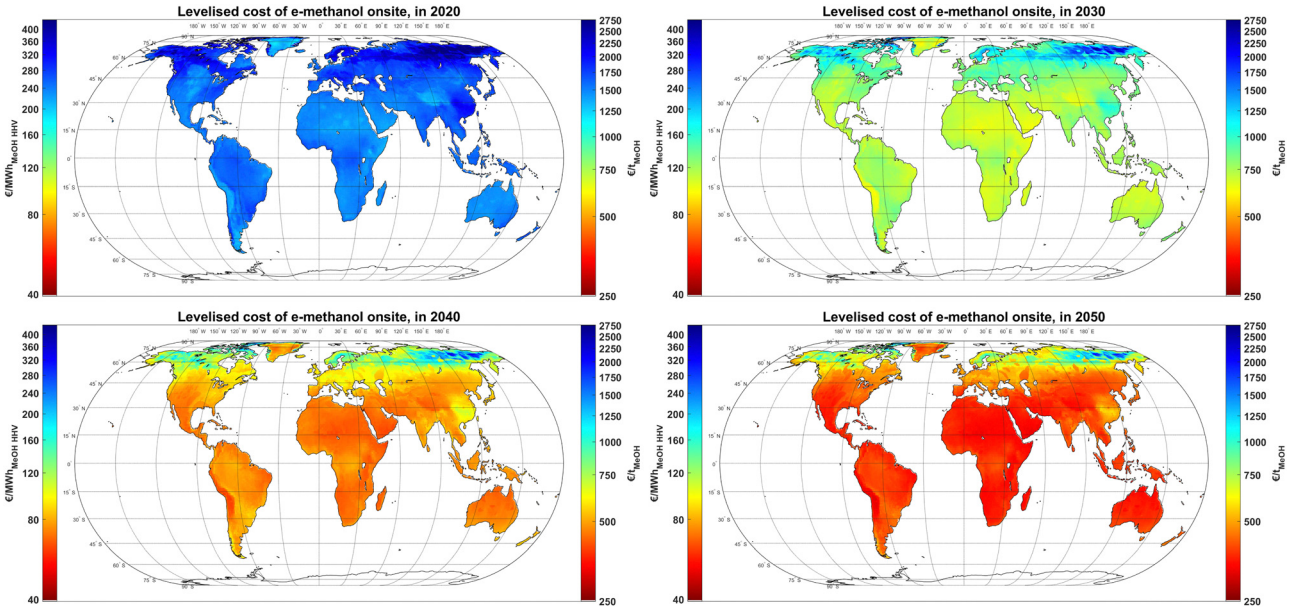

Fig. 4 Levelised cost of e-methanol Onsite in 2020 (top left), 2030 (top right), 2040 (bottom left) and 2050 (bottom right). See Fig. S12 (ESI†) for sub-figures with a customised colour bar range for better visualisation of the lowest cost regions at each cost year.

point source CO_2 are in line with our base results with DAC-based CO_2 for those regions in 2020. They also highlight the impact of flexibility by reporting 20.6–24% and 34.8–32.8% cost savings compared to baseload conservative–optimistic systems in the wind-based and PV-based chosen locations, respectively. Such cost savings by flexible operation were also confirmed by Hank *et al.*[33] Rahmat *et al.*[59] reported on production costs of 2280–2468 € per t_{MeOH} for baseload e-methanol production from point source CO_2, and hybrid PV-wind systems at Friesoythe, Lower Saxony and Stötten, Baden-Württemberg in Germany in 2018. Such costs are even higher than those for a DAC-based e-methanol production of 1600–1800 € per t_{MeOH} for the same region in 2020 in this study, which is due to baseload system configuration, smaller scale and higher hydrogen cost assumptions. Goeppert *et al.*[30] reported 600 USD per t_{MeOH} for a hydrogen cost of 3 USD per kg. However, this seems unrealistic, given that the cost of hydrogen demand (199 kg_{H_2} per t_{MeOH}) alone would be close to 600 USD per t_{MeOH} at this hydrogen price.

The annual e-methanol production at each site is directly linked to the solar and wind potential of the site and applied technology mix. Considering a theoretical 10% area allocation limit for PV and 10% area allocation limit for wind, as shown in Fig. 5, the annual e-methanol production in wind dominated regions could reach 0.2–0.6 $Mt_{MeOH}/1000\ km^2$ (1.3–3.8 $TWh_{MeOH,HHV}/1000\ km^2$), whereas the generation at sites with a mix of PV-wind generation with full usage of the PV area could reach 1.6 to 2.5 $Mt_{MeOH}/1000\ km^2$ (10.2–15.9 $TWh_{MeOH,HHV}/1000\ km^2$) from 2030 to 2050, respectively. This increased production is because, in general, PV-dominated regions have a higher electricity yield than wind per area coverage, and the gap gradually increases as PV installation density improves by 2050.

The theoretical global generation potential of e-methanol increases from about 70 Gt in 2020 to 170 Gt in 2050, as the share of PV in the technology mix and PV areal installation capacity increase and electrolyser and DAC units become more efficient. These potentials far exceed the projected potential global methanol demand of 17 200–20 700 $TWh_{MeOH,HHV}$ (2.71–3.26 Gt) for a full defossilisation of the chemical industry by 2050.[14] As illustrated in Fig. 5, the first 20 Gt_{MeOH} (~10% of global theoretical e-methanol potential) could be produced for a cost of 600–680, 390–430 and 315–350 € per t_{MeOH} (94–107, 61–68 and 50–55 € per $MWh_{MeOH,HHV}$) in 2030, 2040 and 2050, respectively, which could provide enough technical potential for global e-methanol supply.

3.3. Cost distribution at sample locations

The cost distribution of e-methanol production at 7 sample locations are provided in this sub-section, which helps to better grasp the following global analyses. The selected sites include Chilean Patagonia (CHL-PAT), Australia (AUS), USA California (US-CA), Atacama Desert in Chile (CHL-ATA), Germany (DEU), Finland (FIN) and Oman (OMN) with exact coordinates in Table S5 (ESI†). As illustrated in Fig. 6, in 2030, the cost share of the electricity generation system in e-methanol production ranges from 185 € per t_{MeOH} (29 € per $MWh_{MeOH,HHV}$) in the PV-dominated Atacama Desert in Chile to 408 € per t_{MeOH} (64 € per $MWh_{MeOH,HHV}$) in Finland with a PV-wind mix power generation system. The battery system is mainly used in the PV-dominated locations, which adds 20–24 € per t_{MeOH} (3.1–3.8 € per $MWh_{MeOH,HHV}$) to the cost of e-methanol. While the cost of an electricity supply at the PV-dominated regions is the lowest, the share of the non-energetic cost of electrolysers at these locations is the highest at about 130 € per t_{MeOH}

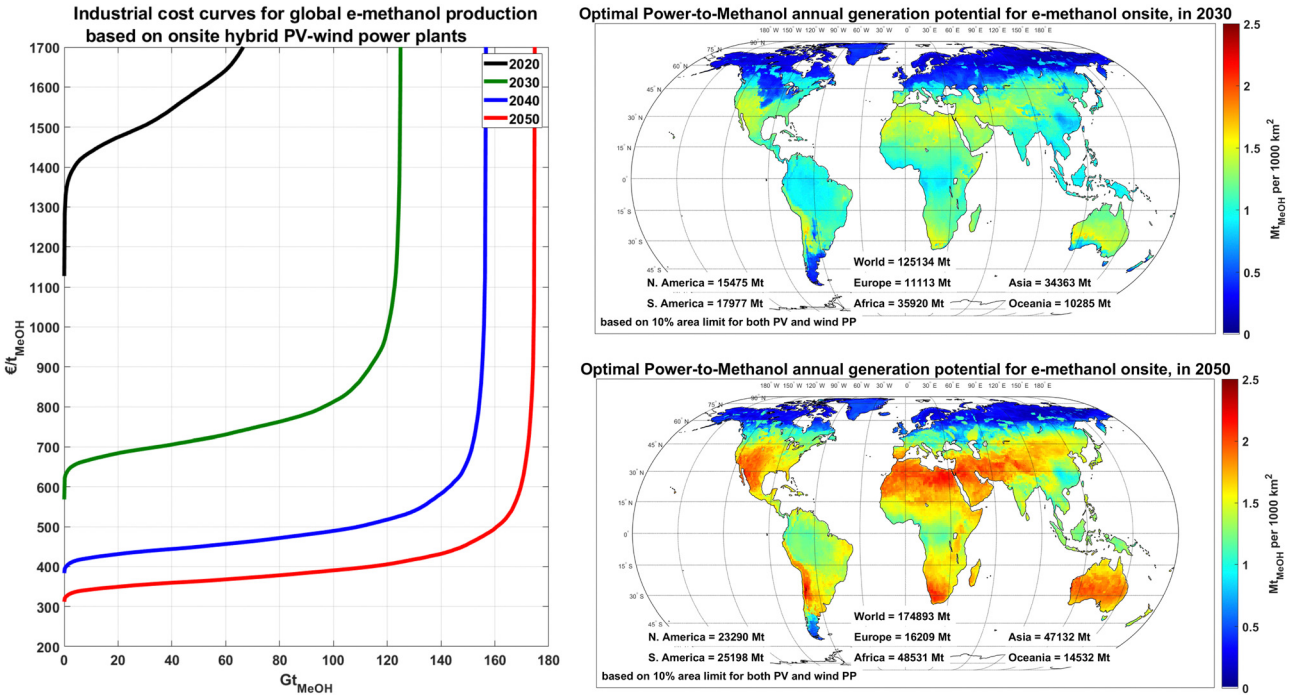

Fig. 5 Power-to-methanol optimal annual generation potential in 2030 (top right) and 2050 (bottom right) with 10% area coverage limit for PV and 10% area coverage limit for wind power plants per 1000 km^2, as well as respective industrial cost curves for the period 2020 to 2050 (left).

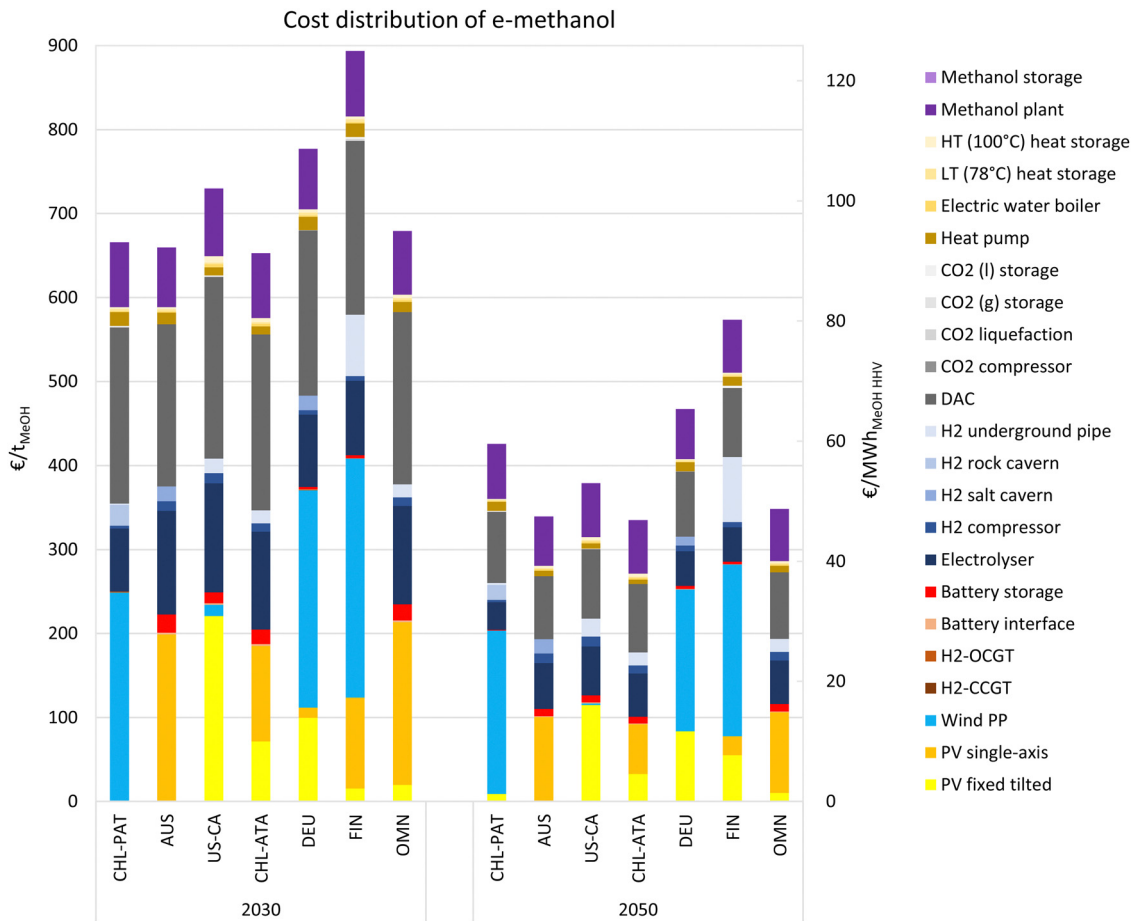

Fig. 6 e-Methanol cost distribution in 2030 and 2050 in selected locations.

(20 € per $MWh_{MeOH,HHV}$) due to the low FLh of the power supply and consequently electrolysers in these locations.

At 193–216 € per t_{MeOH} (30–34 € per $MWh_{MeOH,HHV}$), the non-energetic cost share of DAC units is the second major cost in e-methanol production, and the non-energetic cost of heat generation and supply system could add another 20–25 € per t_{MeOH} (3.1–3.9 € per $MWh_{MeOH,HHV}$) to the cost of e-methanol in 2030. The other major contributor to the cost of e-methanol production is the methanol synthesis plant at 71–81 € per t_{MeOH} (11–13 € per $MWh_{MeOH,HHV}$).

By 2050, the non-energetic cost of DAC declines by about 60% compared to 2030, the sharpest among all considered technologies. A higher cost reduction is observed in PV-dominated regions in general. For example, while Patagonia in Argentina is one of the lowest cost locations in 2030, the plants in Australia, California (US), the Atacama Desert (Chile), and Oman all reach significantly lower e-methanol production costs in 2050, due to the sharper cost reduction of PV and electrolysers compared to wind power. The decline in the cost share of the methanol synthesis plant in the total cost from 2030 to 2050 is due to the lower capex of the synthesis plant gained by economies of scale.

The cost of CO_2 from DAC in a cost optimised Power-to-X system cannot be totally isolated and evaluated, due to shared energy balancing systems and curtailment. Nevertheless, here we attempt to approximate the cost of CO_2 by DAC in the e-methanol plant. In 2030, the non-energetic cost of CO_2-related units (DAC, CO_2 compression and liquefaction units, heat pump, and electric water boiler) stand for 213–241 € per t_{MeOH} in the sample locations. In addition, these units together consume 1211–1811 kWh per t_{MeOH}, which contribute 24–48 € per t_{MeOH} based on an average delivered electricity cost of 17–35 € per MWh (Fig. 3). In total, the energetic and non-energetic cost of CO_2 supply system contribute 237–284 € per t_{MeOH}. 1.46 t_{CO_2} is required for production of 1 tonnes of e-methanol. Accordingly, the cost of CO_2 in 2030 would be 163–195 € per t_{CO_2}. In 2020, the more capex and energy intensive DAC units, together with higher renewable electricity cost, lead to a CO_2 cost of about ~700 € per t_{MeOH} or ~500 € per t_{CO_2}. This highlights the importance of low-cost and sustainable or unavoidable point sources of CO_2, such as pulp and paper mills, waste incinerators, and limestone-based CO_2 from cement production, in lowering the cost of e-methanol production in the next decade at locations with low-cost renewable e-hydrogen production potential.

3.4. Overall efficiency and area demand

The overall efficiency of the power-to-methanol chain was 38–45% in most regions in 2020, which gradually increases to 45–55% in 2050 (Fig. 7). This increase is due to an increase in the efficiency of electrolysers, DAC and batteries, regardless of increasing curtailment over time. In general, the overall efficiency is relatively higher in regions with less seasonality of power supply, such as PV-dominated regions within ±30° latitude, or wind-dominated regions with exceptionally high FLh, such as Patagonia, as well as regions with a complementary role of PV and wind resources such as coastal regions of Western and Northern Europe.

In some parts of the Russian Far East (90°–150°E, 50°–65°N), the overall efficiency declines over time. This is because as electricity generation becomes cheaper over time, higher levels of curtailment in regions with high seasonality of power generation become part of the cost-optimal solution for methanol

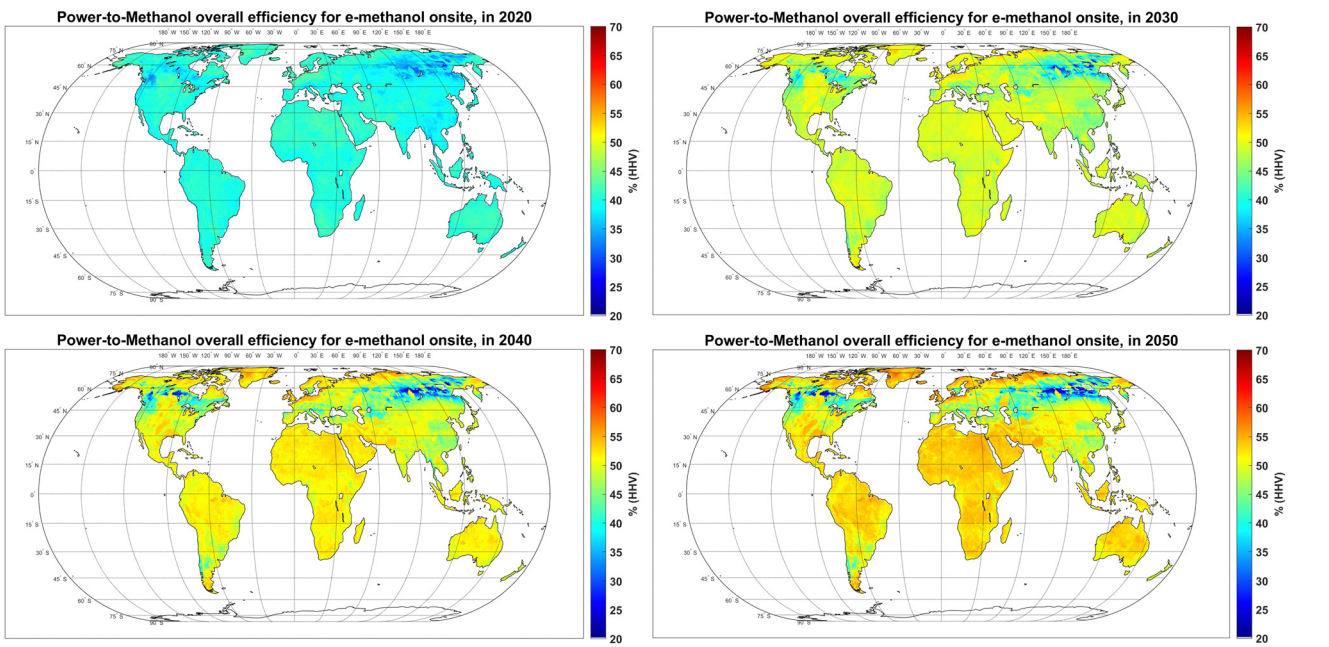

Fig. 7 Power-to-methanol overall efficiency Onsite in 2020 (top left), 2030 (top right), 2040 (bottom left) and 2050 (bottom, right).

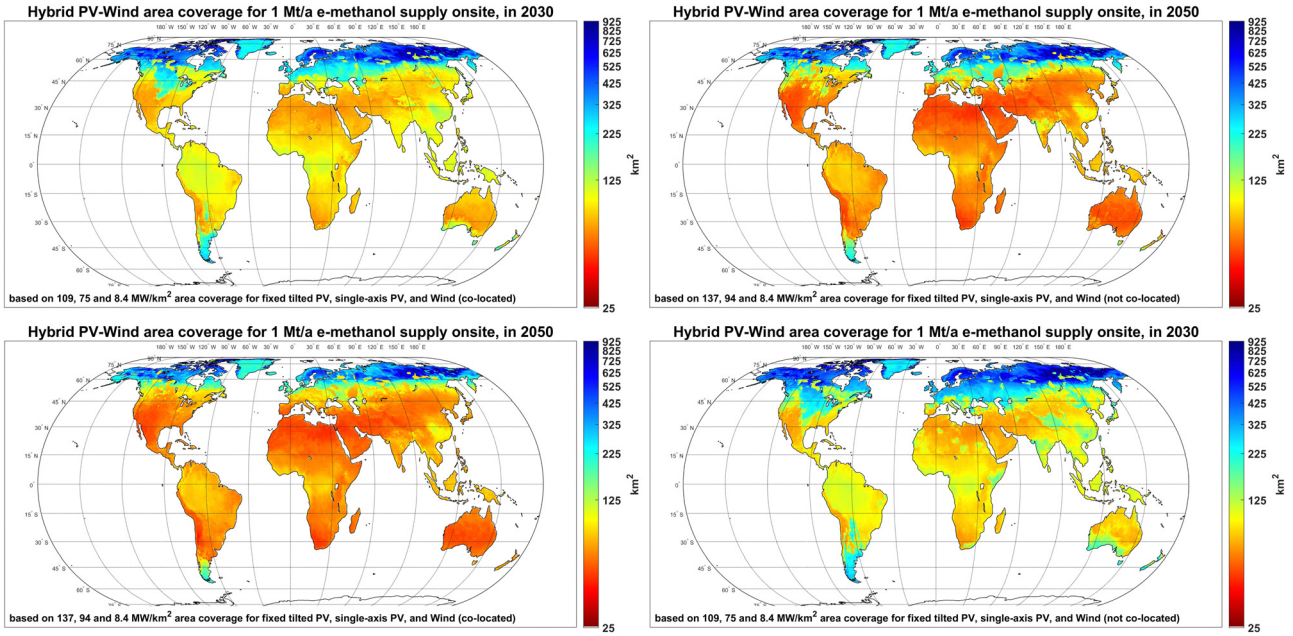

Fig. 8 Area coverage of hybrid PV-wind power plants for 1 Mt per year e-methanol supply in 2030 (left) and 2050 (right) with PV and wind plants not co-located (top) and co-located (bottom).

production (Fig. 2). In other words, higher curtailment levels would become less expensive than other balancing solutions.

The area coverage of hybrid PV-wind systems for 1 Mt per year e-methanol supply in 2030 and 2050 are provided in Fig. 8. The results show that the PV-wind area coverage for 1 Mt per year e-methanol supply in 2030 is 55–500 km^2 in most regions. The lower end of the given range represents PV-dominated regions with high PV FLh, whereas the middle to higher end is associated with wind-dominated or PV-wind mixed systems due to lower installation density and delivered electricity of wind power compared to PV. In regions with a mix of PV and wind power supply, such as Central Europe, the co-location of PV and wind power plants could reduce the gross area coverage for 1 Mt per year e-methanol supply from about 200–350 km^2 to 150–270 km^2. It should be mentioned that the direct area impact of PV and wind power plants is about 50%[60] and 1–2%[61] of their area coverage, respectively, and the rest of the land could be potentially used for other applications. By 2050, the area coverage for 1 Mt per year e-methanol supply in PV-dominated regions declines by about 20% to 45–400 km^2, due to higher PV installation densities. The area coverage reductions in Central Europe could be up to 50% by 2050, as apart from progressive PV installation density, the share of PV in the energy mix increases compared to 2030.

3.5. Flexible operation and relevance of balancing technologies

As discussed in Section 3.3, apart from the power supplying technologies, electrolyser, DAC, and methanol synthesis units have a major impact on the total cost of e-methanol production. As such, their utilisation factor, or FLh, could significantly affect the total cost of the system. As illustrated in Fig. 9, the FLh of electrolysers in PV-dominated regions is within 2600–3200 hours, even though the highest PV FLh is less than 2600 hours (Fig. S1, ESI†). The additional FLh of the electrolyser is not gained by utilisation of batteries (Fig. 2), rather, it is achieved by lowering the size of electrolyser units compared to the PV system with minimal curtailments, as explained extensively in Fasihi and Breyer.[62] Electrolysers are both a capex- and electricity-intensive equipment. With the current cost projections for PV, battery and electrolysers, the cost benefits of higher electrolyser FLh by utilisation of batteries are offset by the increase in the average cost of fed electricity. The electrolyser FLh in regions with a PV-wind mix power supply, such as coastal areas of Western Europe, reaches 5000 hours in 2030, which later decline to less than 4000 hours in 2050 as the share of PV in the power supply increases. The FLh of electrolysers in regions with excellent wind resources, such as Patagonia, could reach 6000 in 2030.

In contrast to electrolysers that follow the availability of a relatively low-cost primary power supply, DAC units exhibit FLh of 7000–8000 hours, regardless of region and year. This high FLh is firstly because DAC units remain a relatively capex-intensive unit in the system from 2020 to 2050. Secondly, the energy demand of the chosen DAC technology is mainly in the form of low temperature (~100 °C) heat,[47] which can be balanced at relatively lower costs compared to the power balancing system required to increase the FLh of electrolysers. High DAC FLh were also reported by Svitnič and Sundmacher[41] for a fully flexible power-to-methanol plant.

At 6700–7700 hours, the FLh of the methanol synthesis plant in 2030 is slightly lower than the FLh of DAC units, suggesting that a CO_2 storage system is required, which is discussed later

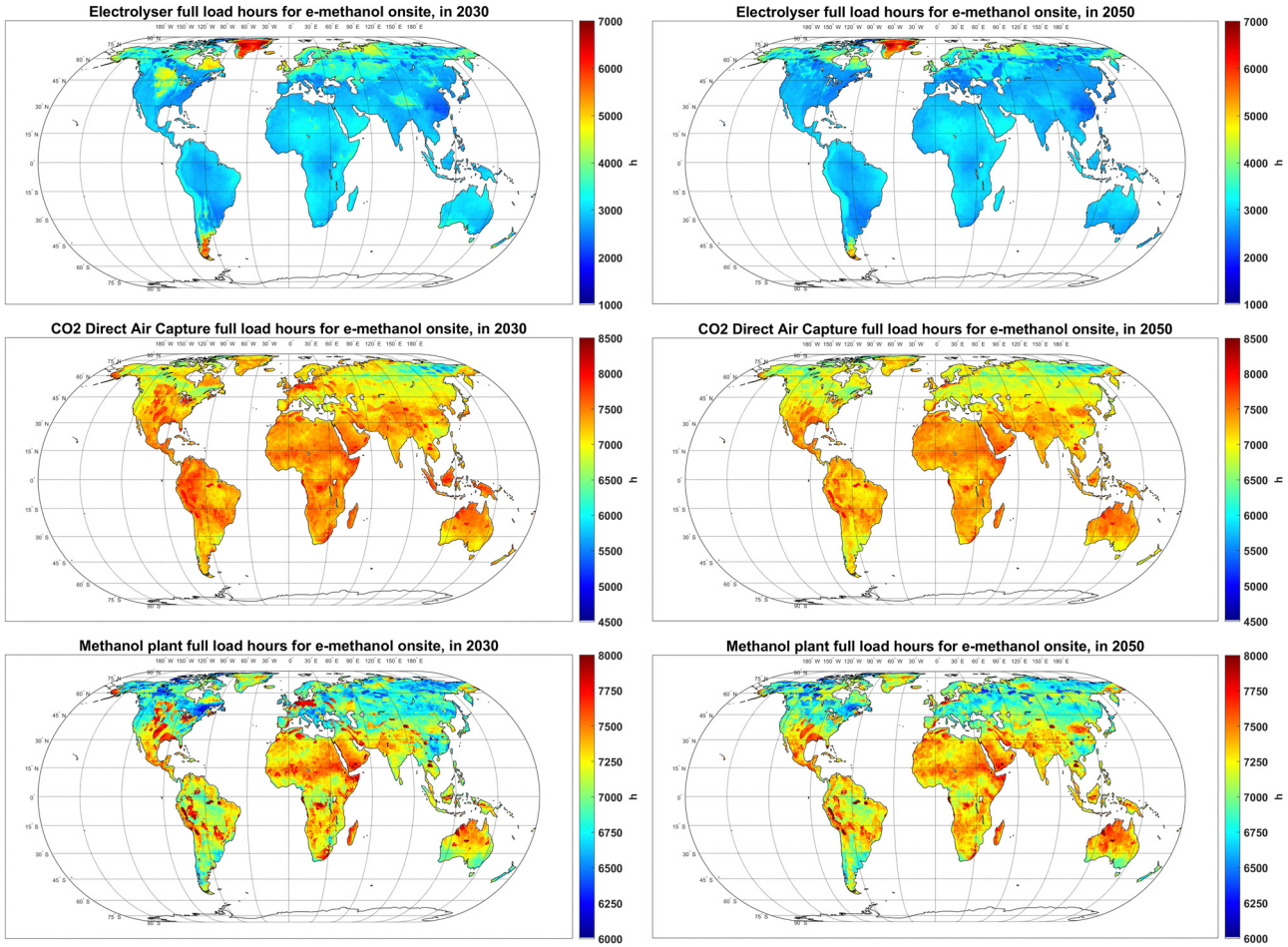

Fig. 9 Full load hours of electrolyser (top), CO_2 direct air capture (centre) and methanol plant (bottom) in 2030 (left) and 2050 (right).

in this section. The FLh of methanol plants are exceptionally high in regions with access to relatively low-cost salt cavern hydrogen storage, which indicates that the high cost of close-to-baseload hydrogen supply in other regions is the limiting factor for achieving higher FLh for methanol synthesis plants. Hank *et al.*[33] also report on benefits of flexible operation and lower FLh on the production cost.

The lower FLh of electrolyser units compared to the FLh of the methanol synthesis unit results in over production of hydrogen at peak hours. The results in Fig. 10 show that, to balance the hydrogen supply from electrolysers, the required hydrogen compressor capacity would be 55–70% of the capacity of the electrolyser units in most PV-dominated regions. The capacity ratio of compressors to electrolysers could be beyond 80% in some PV-dominated regions with the seasonality of PV power supply, such as British Columbia and Manitoba in Canada.

The optimal size of the hydrogen storage system is affected by the seasonality of hydrogen generation and available hydrogen storage options. For a 1 Mt per year e-methanol supply in 2030, the hydrogen storage capacity in PV-dominated regions at latitudes below 30°N with no access to salt or rock cavern hydrogen storage is mainly between 10–20 $GWh_{H_2,HHV}$, while the capacity of the hydrogen storage system for locations with access to rock cavern and salt cavern storage in the same region could reach to 100 and 1000 $GWh_{H_2,HHV}$, respectively, due to their lower capex. A 1 Mt per year e-methanol plant in wind-dominated regions limited to underground pipe hydrogen storage at latitudes above 45°N would require about 100 $GWh_{H_2,HHV}$ of hydrogen storage, which is 5 to 10 times higher than that in PV-dominated regions. Separate global maps for the capacity of each hydrogen storage option are provided in Fig. S7 (ESI†).

Regardless of the two orders of magnitudes difference in the capacity of hydrogen storage by location, the annual throughput of the hydrogen storage systems is barely affected by its size and mostly by the FLh of the electrolyser units. For example, for a 1 Mt per year e-methanol supply in 2030, only 20–30% of required hydrogen is stored prior to consumption in 200–300 $GWh_{H_2,HHV}$ storage systems in Northern Germany with about 4500 FLh of electrolysers and access to a salt cavern. Conversely, in Southern Europe, where electrolysers' FLh is below 3000 hours, up to 60% of hydrogen production is stored prior to consumption in 10–20 $GWh_{H_2,HHV}$ underground pipe systems. This high storage level is achieved by almost daily full charge and discharge of the storage system.

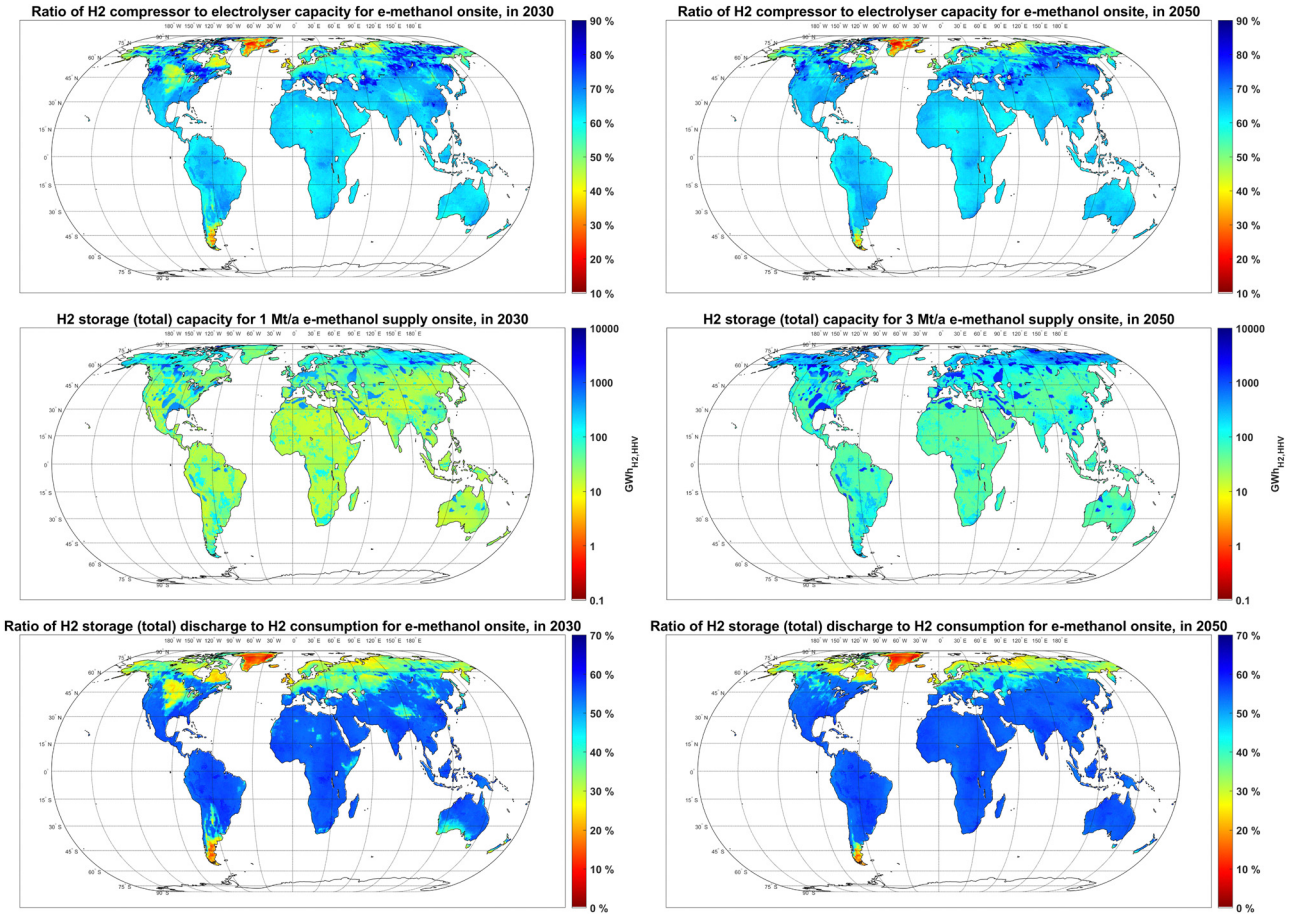

Fig. 10 Relevance of hydrogen balancing technologies, including ratio of H_2 compressor to electrolysers capacity (top), total hydrogen storage capacity (centre), and ratio hydrogen supplied by storage options to the total hydrogen consumption (bottom), in 2030 (left) and 2050 (right).

The significantly smaller maximum hourly charge or discharge rate of salt caverns ($\sim$0.42% h^{-1}) compared to the underground pipe ($\sim$16.7% h^{-1}) contributes to higher installed capacities of salt cavern hydrogen storage compared to underground pipes. In other words, to maintain equal hourly maximum charge or discharge capacity, a 40 times larger salt cavern hydrogen storage capacity is required compared to for the underground pipe system. Meanwhile, as the capex of underground pipe systems is about 30 times higher than those for salt cavern storage, adding more underground pipe system capacity could be part of the cost-optimised solution compared to the salt cavern to increase the storage system's overall charge or discharge capacity. This condition is observed for example in regions suitable for salt cavern in Peru (Fig. S7, ESI†).

The power-to-methanol system in regions with seasonality of power (such as some regions at latitudes above 45°N) and consequently hydrogen production with no access to low-cost hydrogen storage can avoid high costs of seasonal hydrogen balancing by part load operation of the semi-flexible methanol plant in the low-power season, as shown in Fig. S8 (ESI†) for a sample location in Northeast Canada (49.95°N, 75.15°W). This semi-flexible production reduces the overall FLh of the methanol synthesis plant to 6000–6700 hours in these regions, compared to 7000–7700 FLh in sunbelt regions with less seasonality of PV power supply regardless of lower electrolyser FLh that could be more easily balanced by smaller underground hydrogen pipe capacities.

By 2050, more regions become PV-dominated with lower electrolyser FLh, which increases the role of hydrogen storage, such as in Patagonia and Western Australia. The FLh of other components such as heat pump and electric water boiler are provided in the ESI,† Fig. S11.

Heat pumps supply 50–90% of the heat demand of DAC units in power-to-methanol systems, and the remaining 10–50% is supplied by electric water boilers in most regions, as illustrated in Fig. 11. One exception is the Atacama Desert, where electric water boilers could become the main heat supplier in 2050, as the electricity generation cost declines to 7 € per MWh (Fig. S3, ESI†), which makes the efficiency gain by heat pumps less relevant compared to their higher capex.

Up to 50% of the waste heat from electrolysers is used as a heat source for heat pumps in 2030. Even though the heat demand of DAC units declines by 26% from 2030 to 2050, a higher ratio of waste heat from electrolysers (up to 80%) is used as a heat source for heat pumps in 2050. This ratio increases since the absolute amount of utilisable waste heat declines

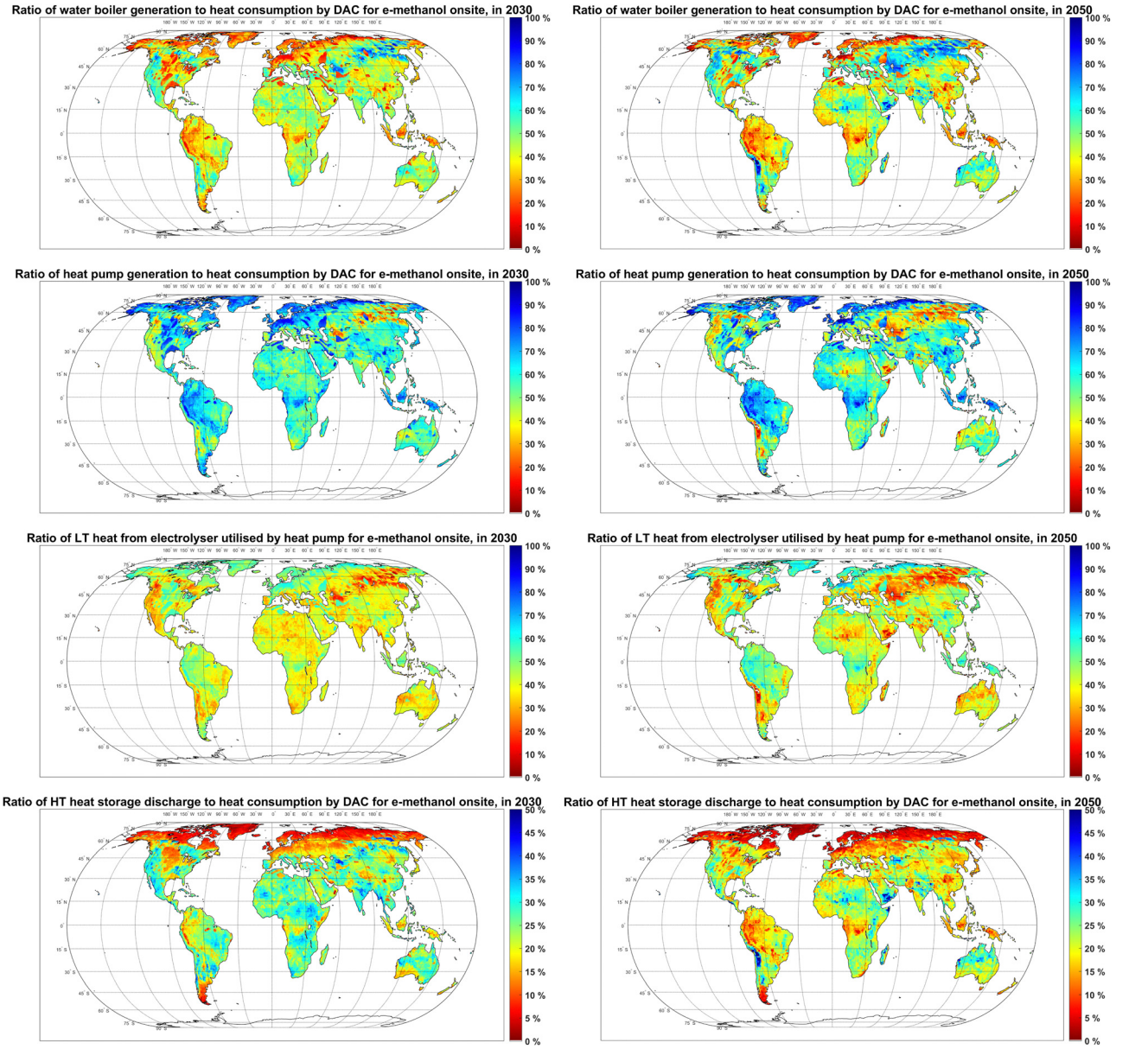

Fig. 11 Relevance of heat supplying and balancing technologies, including ratio of high temperature heat supply by electric water boiler (top), ratio of high temperature heat supply by heat pump (upper centre), ratio of low temperature heat from electrolyser utilised by heat pump (lower centre), and ratio of high temperature heat storage discharge to total heat consumption by DAC (bottom), in 2030 (left) and 2050 (right).

by 32% as the electrolyser efficiency also increases from 2030 to 2050.

Up to 35% of generated high temperature heat is stored prior to utilisation by DAC units in 2030, which declines by 5–10 percentage points by 2050. Regions with higher shares of heat generation by heat pumps (such as Northern regions) can be observed to have a relatively lower high temperature heat storage throughput. This characteristic is because heat pumps in the Northern region mostly have comparable FLh to those for methanol plants (Fig. S11 (ESI†) and Fig. 9), which is higher than the FLh of electric water boilers (Fig. S11, ESI†) in a cost-optimised system due to heat pumps higher capex. The higher availability rates of power generation for minor consumers in the PV-wind mixed systems and the relatively low FLh of heat pumps and methanol plants in the Northern region lead to less demand for batteries as well (Fig. 2).

As shown in Fig. S10 (ESI†), the role of CO_2 balancing technologies in power-to-methanol systems is limited, as both DAC and methanol synthesis plants operate at high FLh (Fig. 9). Gaseous CO_2 compression and storage can be observed to have no significant role in the cost-optimised balancing of the CO_2 supply. On the other hand, the hourly capacity of CO_2 liquefaction units in most regions could be up to 8% of DAC capacity, balancing up to 4% of the annual CO_2 consumption in

2030. By 2050, the operating time and capacity of DAC and methanol units align in more regions, which eliminates the need for CO_2 balancing technology in the respective regions.

3.6. Cost comparison of e-methanol and conventional methanol production

In the past decade, the market price of conventional methanol has been mainly within 200–400 € per tonne (31–63 € per $MWh_{MeOH,HHV}$), as shown in Fig. 12. The results of this research show that e-methanol production cost could reach this price range by 2040, providing the possibility to defossilise methanol production without increasing consumer prices. However, if e-methanol production develops to gain considerable shares in the market, it is expected that conventional methanol and e-methanol compete for lower prices, making the cost comparison more relevant.

The capex of a large-scale conventional NG-based methanol plant is estimated at 804 € per (t_{MeOH} per year) based on cost data from Natgasoline's 1.9 Mt per year greenfield plant in Beaumont, US.[63] Considering a generic fixed opex of 4% and a variable opex of 15 € per t_{MeOH},[31] the cost of methanol production at a NG price range of 1–17 USD per MBtu (2.8–48.4 € per MWh_{NG}) is provided in Fig. 12.

Today, NG-based methanol plants consume about 33.4–36.5 GJ_{NG} per t_{MeOH},[31,64] while the best practice is 31.5 GJ_{NG} per t_{MeOH}.[64] 32 GJ per t_{MeOH} NG consumption would have a carbon content of about 0.52 t_C, of which 0.375 t_C is stored in methanol, while the remaining 0.145 t_C is lost as 0.532 t_{CO_2} in the NG combustion process. The actual emissions from methanol consumption depend on its end use and state (*e.g.*, carbon stored in products with long lifetime or released into the atmosphere in the form of CO_2, CH_4, *etc.*). Here, we assume that all carbon in methanol or its derivatives would end up in the atmosphere in the form of CO_2 at the end of their lifetime. Thus, conventional NG-based methanol production would have a CO_2 emission of 1.92 t_{CO_2} per t_{MeOH}, excluding the CO_2 and methane emissions in the NG supply chain.

As illustrated in Fig. 12, the production cost of NG-based methanol is highly affected by NG prices and increases from 146 to 551 € per t_{MeOH} (23–87 € per $MWh_{MeOH,HHV}$) for a NG price of 1 to 17 USD per MBtu (2.8–48.4 € per MWh_{th}), respectively. With almost 2 t_{CO_2} emissions per tonne of methanol production, the cost of conventional methanol is also highly dependent on the CO_2 emissions pricing and will increase by 383 € per t_{MeOH} for a CO_2 emission price of 200 € per t_{CO_2}.

The results show that, in 2020, e-methanol was not cost-competitive with NG-based methanol for any combination of NG and CO_2 emissions price. In 2030, e-methanol could reach fuel parity with conventional methanol for a NG and CO_2 emissions price combination of 15.5 USD per $MBtu_{NG}$ and 50 € per t_{CO_2}, or 12 USD per $MBtu_{NG}$ and 100 € per t_{CO_2}, or 8 USD per $MBtu_{NG}$ and 150 € per t_{CO_2}, or 4.8 USD per $MBtu_{NG}$ and 200 € per t_{CO_2}. While NG prices over 15 USD per MBtu and CO_2 emissions prices over 80 € per t_{CO_2} were experienced in the European market in 2022,[66] stabilisation at such prices seems unlikely. Similarly, CO_2 emissions prices in the European Union Emissions Trading System have sharply increased since 2021 but have remained relatively stable at prices over 60 € per t_{CO_2}.

By 2040, e-methanol could be cost competitive at NG prices over 11 or 3.5 USD per MBtu (31 or 10 € per MWh_{th}) with zero or 100 € per t_{CO_2} emissions cost, respectively, with the latter

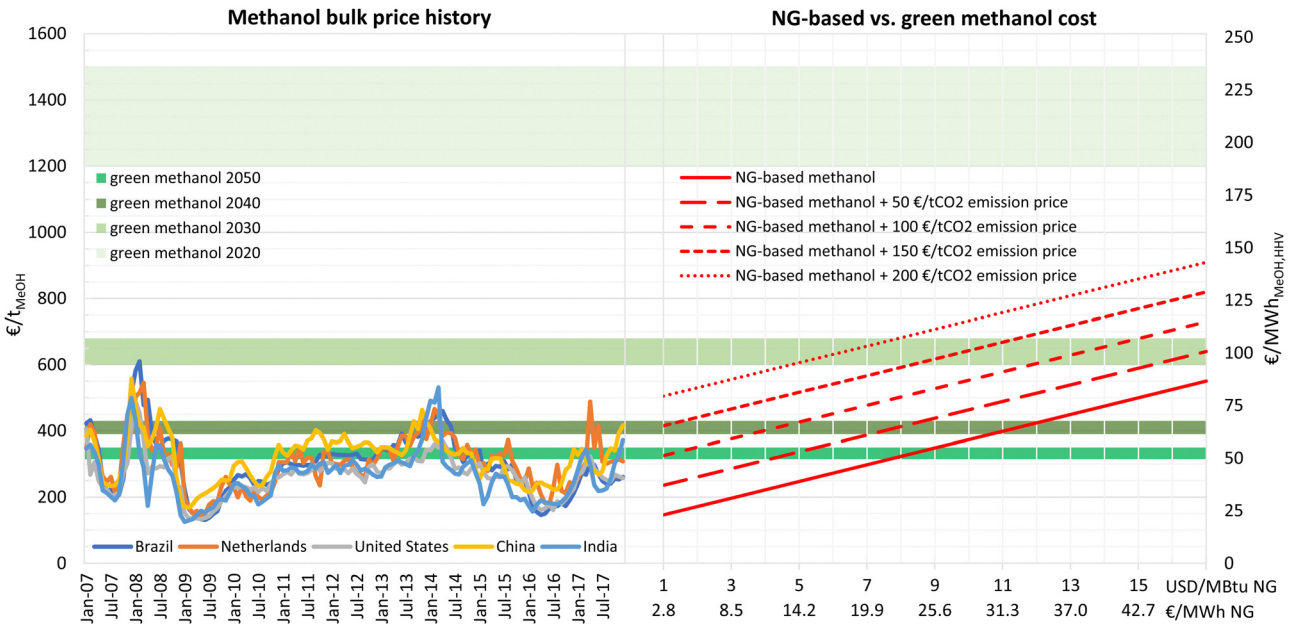

Fig. 12 History of methanol bulk market prices (left) and NG-based *vs.* green methanol cost for varying natural gas and CO_2 emission prices (right). Green methanol cost range at best sites with 20 Gt_{MeOH} per year cumulative production potential. Methanol price history is based on data from Intratec[65] and a 1.2 € per USD exchange rate.

scenario being more likely. For a CO_2 emissions price of 150 € per t_{CO_2}, e-methanol would be cost competitive by 2040 at any NG price. By 2050, e-methanol could be competitive for NG prices over 7.5 USD per MBtu (21 € per MWh_{th}) at no CO_2 emissions price or at NG prices as low as 1 USD per MBtu (2.8 € per MWh_{th}) at 150 € per t_{CO_2} CO_2 emissions price. This result indicates that, considering low costs of NG at major producers, governmental policies such as CO_2 emissions pricing (*e.g.* the European carbon border adjustment mechanism) are essential to make e-methanol a global substitute for conventional methanol by 2050.

3.7. Potential competing and complementary role of e-methanol and e-ammonia

Apart from the key role of e-methanol in defossilisation of the chemical industry, it may compete with e-ammonia as potential sustainable fuels for long-range marine sector. The energetic cost of e-methanol at the lowest cost regions in 2020 is 180–220 € per $MWh_{MeOH,HHV}$, which is about double the e-ammonia production cost of 90–110 € per $MWh_{NH_3,HHV}$ (Fig. S13, ESI†). By 2050, as the cost and energy efficiency of DAC plants improve, together with economies of scale by deployment of larger methanol plants, the gap between the production cost of e-methanol and e-ammonia further declines to about 10 € per $MWh_{th,HHV}$ (or ~25%) for 50–55 € per $MWh_{MeOH,HHV}$ and 39–45 € per $MWh_{NH3,HHV}$. However, apart from the cost, the selection of potential future sustainable marine fuel is affected by other factors, such as safety, functionality, and short- and long-term scalability, as further discussed in Section S4 (ESI†).

The waste heat from e-ammonia production could potentially be used as a heat source for DAC units in the e-methanol production chain, as explained in Section S5 (ESI†). The co-production of 1 Mt per year of e-methanol and 1 Mt per year of e-ammonia in 2030 could reduce the cost of e-methanol by 20–40 € per t_{MeOH} (2–4%), as illustrated in Fig. S15 (ESI†). The cost reduction by heat integration in most regions could be increased to 30–50 € per t_{MeOH} (4–6%) by reducing the size of e-methanol supply to 0.5 Mt per year in the hybrid system. In 2050, combining the reference plant for 3 Mt per year e-methanol supply with 1 Mt per year ammonia supply plant would only reduce the cost of e-methanol supply by about 6–14 € per t_{MeOH} (1–2%) due to lower availability of waste heat per tonne of e-methanol. Elevating the share of waste heat supply per tonne of e-methanol by down-scaling the integrated e-methanol plant from 3 to 1 Mt per year supply in 2050 would widen the cost reduction to 2–18 € per t_{MeOH} (0.5–2%) compared to the solo 3 Mt per year methanol supply system in most parts of the world. This is due to counter impact of economies of scale and importance of external heat availability depending on the regional system configuration. For example, it is observed that Northern regions (above 50° latitude) would have a greater cost reduction, while central regions would experience less cost reduction in absolute value (€ per t_{MeOH}).

3.8. Limitations and sensitivity analyses

A series of sensitivity analyses are performed on units or factors with major uncertainty or impact on e-methanol production cost in 2030.

The WACC for new investments varies significantly by regional conditions. However, due to uncertainties with the correct relative value of regional WACC, especially for future projects, a global unified WACC of 7% was used in this study. As shown in Fig. S16 (ESI†), a ±2 percentage points deviation in WACC affects the cost of e-methanol production by 13–15% compared to the Base Cost Scenario (BCS) in most regions. The impact of a WACC change on the overall cost is relatively higher in systems with components with longer lifetime. For example, increasing the WACC from 7% to 9% would increase the respective LCOE from wind and PV power plants with 25 and 35 lifetimes by 15.1% and 16.5%, respectively.

Electrolysers are a core technology in Power-to-X systems. Due to uncertainties regarding their cost by time, region, and supplier, a High-Cost Scenario (HCS) is defined in which, compared to the BCS, the capex and fixed opex of electrolyser have increased by 31% in 2020, followed by half deployment by each next time step and consequently lower impact of the learning rate in the HCS, resulting in 56%, 59% and 60% higher capex in 2030, 2040 and 2050, respectively (Table S8, ESI†). As illustrated in Fig. S17 and S18 (ESI†), in 2020, the production cost of e-methanol would increase by 40–90 € per t_{MeOH} (6–14 € per $MWh_{MeOH,HHV}$) or 4–6% in the HCS compared to in the BCS, of which the higher end is related to PV-dominated regions with higher capacities of electrolysers. In 2030, while the absolute cost increase remains at 40–90 € per t_{MeOH}, the relative cost difference increases by 4–11%, as e-methanol (BCS) is lower in cost than in 2020. The absolute cost difference declines to 20–40 € per t_{MeOH} by 2050, equal to about 10% cost increase in PV-dominated regions. The higher cost electrolyser is also observed to have 50–1000 hours higher FLh in the cost optimised system to lower the total installed capacity and the cost through higher utilisation rate (Fig. S19, ESI†).

While first commercial and industrial scale DAC plants are being deployed, DAC plants have the lowest technology readiness level among all technologies applied in the power-to-methanol supply chain. The techno-economic projections in the BCS outline a possible future development for DAC similar to comparable technologies. However, the possibility exists that DAC will not develop according to expectations within the given timeframe. In addition, DAC productivity and energy demand is affected by ambient temperature and relative humidity, which differ by time and location.[67–69] The current study is limited in that regard as it is based on nominal annual average productivity and energy demand in test locations. In the BCS, DAC experiences a major capex reduction and energy efficiency gain by 2030. Thus, a HCS is provided for DAC, in which the cost and energy improvements by 2030 are half of those considered in the BCS, and the cost and energy demand by 2050 reach those for BCS in 2030. The results, shown in Fig. S20 (ESI†), indicate that the HCS would mainly increase the cost of e-methanol production by 190–260 € per t_{MeOH} (30–41 € per $MWh_{MeOH,HHV}$

or 16–30%), in 2030. Regions least affected are those with high DAC FLh (and consequently lower installed capacity of DAC) and low LCOE (and consequently low heat generation cost). In 2050, the HCS DAC would increase the cost of e-methanol production by 10–40 € per t_{MeOH} (1.6–6.3 € per $MWh_{MeOH,HHV}$ or 10–35%).

Generic sensitivity analyses are performed on solar PV, wind power and methanol plants by a ±10% deviation in the capex and fixed opex compared to the BCS (Table S8, ESI†). The sensitivity analyses presented in Fig. S21 (ESI†) show that a 10% change in the capex and opex of the PV system would affect the cost of e-methanol production by up to ~4% in PV-dominated regions. The same level of impact is observed in the wind-dominated regions such as Patagonia and Northern Europe. A 10% change in the capex and non-energetic opex of methanol synthesis plant would affect the total cost of e-methanol production by about 1% in 2030.

Finally, the magnitude of benefits of the cost-optimised hybrid PV-wind system for e-methanol production over PV-only or wind-only systems for the year 2030 are illustrated in Fig. S22 (ESI†). A PV-only scenario would double the cost of e-methanol production in Northern Europe and increase it by up to 1000 € per t_{MeOH}. This sharp increase in cost is due to strong seasonality of solar energy in Northern Europe and the need for large-scale hydrogen and CO_2 storage to maintain the defined minimum operational capacity of 50% for the methanol synthesis unit during winter. The regions between ±45° latitude are mostly not affected by a PV-only scenario, as the cost-optimised configuration is also fully based on PV. A wind-only scenario, on the other hand, would increase the cost of e-methanol almost everywhere except for some parts of Patagonia where wind power is the sole source of electricity in the optimised system. The cost increase of a wind-only scenario in 2030 is mainly 50–400 € per t_{MeOH}, equivalent to a 10–90% cost increase. Regions close to the equator are more negatively affected by a wind-only scenario due to the low wind energy potential in rainforest areas.

4. Conclusions

In this study, semi-flexible power-to-methanol plants were modelled as islanded systems, and their cost-optimised performance based on hourly power supply from hybrid PV-wind power plants and balancing technologies in a 0.45° × 0.45° spatial resolution were evaluated for respective projected techno-economic specifications of components for the years 2020, 2030, 2040 and 2050.

The results show that, by 2030, the cost-optimised configuration of the power supply would be mainly PV-dominated in most parts of the world except for Patagonia, Northern and Western Europe, as well as the Northern US.

For a weighted average cost of capital of 7%, the least cost e-methanol production at best sites in 2020 is in the range of 1200–1500 € per t_{MeOH} (189–236 € per $MWh_{MeOH,HHV}$), which is significantly above the average market prices of 200–400 € per t_{MeOH} (31–63 € per $MWh_{MeOH,HHV}$) in the last decade. The cost of e-methanol in 2020s is strongly affected by the high cost of early-stage DAC. This highlights the role of low-cost point source CO_2 to lower the cost of CO_2-to-methanol in early years, wherever sustainable or unavoidable CO_2 could be co-located with low-cost electricity for hydrogen production. By 2030, the production cost of e-methanol in the best regions declines to 600–680 € per t_{MeOH} (94–104 € per $MWh_{MeOH,HHV}$), which would be achievable in all continents and close to the highest European methanol market prices in recent years. e-Methanol production costs decline to 390–430 € per t_{MeOH} (61–68 € per $MWh_{MeOH,HHV}$), by 2040, with the Atacama Desert being the lowest cost location in the world. By 2050, production costs decline to 315–350 € per t_{MeOH} (50–54 € per $MWh_{MeOH,HHV}$) in all continents, making e-methanol production cost well within the current market price range, but higher than the production cost of NG-based methanol for NG prices lower than 7.5 USD per MBtu (21 € per MWh_{th}) without any CO_2 pricing. This result emphasises the importance of CO_2 emissions pricing, as well as early support for DAC and point sourced CO_2-to-methanol plants, for ramping e-methanol on relevant scales. For an overall CO_2 emission of about 2 t_{CO_2} per t_{MeOH} and 100 € per t_{CO_2}, e-methanol could be cost competitive already by 2040.

The global theoretical annual generation potential of e-methanol is three orders of magnitude more than its current demand, which provides the options for local production and supply, or import from the lowest cost regions. In addition, it provides the possibility of expanding the e-methanol market, where methanol can serve as the main feedstock for chemical industry, as fuel for long-range marine transport, and indirectly as fuel for aviation *via* the e-methanol-to-kerosene route.

The energetic costs of e-methanol remain higher than those for e-ammonia, but the gap declines to about 10 € per $MWh_{th,HHV}$ (or ~25%) in 2050. e-Methanol and e-ammonia plant integration for waste heat utilisation could also reduce the cost of e-methanol by 20–40 € per t_{MeOH} (4–6%) in 2030, depending on location and supply ratio of e-methanol and e-ammonia. By 2050, the benefits of system integration decline to 2–18 € per t_{MeOH} (0.5–2%) of the solo e-methanol plant cost.

The sensitivity analyses show that e-methanol production cost in 2030 is mostly affected by a slower advancement in direct air capture technology (16–30% higher e-methanol cost for realisation of half of the projected advancement by 2030), followed by a regional weighted average cost of capital (13–15% cost change for a ±2 percentage points deviation from the unified weighted average cost of capital), and higher cost of electrolysers (4–11% higher e-methanol cost for 56% higher cost electrolyser).

e-Methanol could be produced cost effectively at scale by 2040 (or earlier *via* fossil CO_2 pricing), which can enable it to be a key feedstock for defossilisation of the chemical industry.

Abbreviations

BCS	Base cost scenario
CH_3OH	Methanol
CRI	Carbon Recycling International

Comp.	Compressor
DAC	Direct air capture
e-methanol	Electricity-based methanol
FLh	Full load hours
GHG	Greenhous gas
H_2-CCGT	Hydrogen-fuelled combined cycle gas turbine
H_2-OCGT	Hydrogen-fuelled open cycle gas turbine
HCS	High-cost scenario
HHV	Higher heating value
HT	High temperature
LT	Low temperature
MeOH	Methanol
PEM	Proton exchange membrane
PV	Photovoltaics
TED	Total electricity demand
WACC	Weighted average cost of capital

Conflicts of interest

The authors declare no competing interests.

Acknowledgements

The authors gratefully acknowledge the funding of Shell Global Solutions International B.V. (Agreement No. CW308144) for the ''100% Renewable Energy System Models – Global Fuels and Bulk Chemicals Trading'' project and the public funding of Business Finland for the 'P2XENABLE' project under the number 8588/31/2019. The authors would like to thank Alexander van der Made and FU Xiao and their team at Shell for the valuable discussions. We also thank Gabriel Lopez for proofreading.

References

1 Statista, Distribution of primary petrochemical consumption worldwide in 2022, by type, **https://www.statista.com/statistics/1319374/petrochemical-consumption-share-by-type-globally/**, accessed 15 June 2023.
2 Research Dive, Methanol Market Report, 2022.
3 M. Alvarado, *The changing face of the global methanol industry*, 2016, vol. 3.
4 S. A. Al-Sobhi, A. AlNouss and M. Alhamad, *Comput. Aided Chem. Eng.*, 2021, vol. 50, pp. 1827–1832.
5 Statista, Production of methanol worldwide from 2017 to 2022, **https://www.statista.com/statistics/1323406/methanol-production-worldwide/**, accessed 13 June 2023.
6 J. Penman, M. Gytarsky, T. Hiraishi, W. Irving and T. Krug, *2006 IPCC Guidelines for National Greenhouse Gas Inventories – A primer*, 2008.
7 IPCC, *Summary for Policymakers. Global Warming of 1.5 °C. An IPCC Special Report on the impacts of global warming of 1.5 °C above pre-industrial levels*, 2018.
8 United Nations, *Adoption of the Paris Agreement, Proposal by the President, Draft decision*, 2015.
9 [IRENA] – International Renewable Energy Agency, *Renewable Power Generation Costs in 2022*, Abu Dhabi, 2023.
10 S. Chowdhury, Y. Kumar, S. Shrivastava, S. K. Patel and J. S. Sangwai, *Energy Fuels*, 2023, **37**, 119416.
11 Carbon Recycling International, The Shunli CO2 -To-Methanol Plant: Commercial Scale Production in China, **https://www.carbonrecycling.is/projects-shunli**, accessed 9 June 2023.
12 A. Kätelhön, R. Meys, S. Deutz, S. Suh and A. Bardow, *Proc. Natl. Acad. Sci. U. S. A.*, 2019, **166**, 11187–11194.
13 Á. Galán-Martín, V. Tulus, I. Díaz, C. Pozo, J. Pérez-Ramírez and G. Guillén-Gosálbez, *One Earth*, 2021, **4**, 565–583.
14 G. Lopez, D. Keiner, M. Fasihi, T. Koiranen and C. Breyer, *Energy Environ. Sci.*, 2023, **16**, 2879–2909.
15 N. Gray, S. McDonagh, R. O'Shea, B. Smyth and J. D. Murphy, *Adv. Appl. Energy*, 2021, **1**, 100008.
16 K. Atsonios, J. Li and V. J. Inglezakis, *Energy*, 2023, **278**, 127868.
17 S. Bube, N. Bullerdiek, S. Voß and M. Kaltschmitt, *Fuel*, 2024, **366**, 131269.
18 G. A. Olah, A. Goeppert and G. K. S. Prakash, *Beyond Oil and Gas: The Methanol Economy*, 2nd edn, 2009.
19 G. A. Olah, *Angew. Chem., Int. Ed.*, 2005, **44**, 2636–2639.
20 A. Sonthalia, N. Kumar, M. Tomar, V. Edwin Geo, S. Thiyagarajan and A. Pugazhendhi, *Clean Technol. Environ. Policy*, 2023, **25**, 551–575.
21 S. K. Kar, S. Harichandan and B. Roy, *Int. J. Hydrogen Energy*, 2022, **47**, 10803–10824.
22 C. Breyer, G. Lopez, D. Bogdanov and P. Laaksonen, *Int. J. Hydrogen Energy*, 2024, **49**, 351–359.
23 T. Galimova, M. Ram, D. Bogdanov, M. Fasihi, S. Khalili, A. Gulagi, H. Karjunen, T. N. O. Mensah and C. Breyer, *J. Clean Prod.*, 2022, **373**, 133920.
24 T. Galimova, M. Ram, D. Bogdanov, M. Fasihi, A. Gulagi, S. Khalili and C. Breyer, *Renewable Sustainable Energy Rev.*, 2023, **183**, 113420.
25 É. S. Van-Dal and C. Bouallou, *J. Clean Prod.*, 2013, **57**, 38–45.
26 B. Anicic, P. Trop and D. Goricanec, *Energy*, 2014, **77**, 279–289.
27 V. Dieterich, A. Buttler, A. Hanel, H. Spliethoff and S. Fendt, *Energy Environ. Sci.*, 2020, **13**, 3207–3252.
28 A. Tremel, P. Wasserscheid, M. Baldauf and T. Hammer, *Int. J. Hydrogen Energy*, 2015, **40**, 11457–11464.
29 Carbon Recycling International, Our Projects, **https://www.carbonrecycling.is/projects**, accessed 16 June 2023.
30 A. Goeppert, M. Czaun, J. P. Jones, G. K. Surya Prakash and G. A. Olah, *Chem. Soc. Rev.*, 2014, **43**, 7995–8048.
31 M. Pérez-Fortes, J. C. Schöneberger, A. Boulamanti and E. Tzimas, *Appl. Energy*, 2016, **161**, 718–732.
32 S. Michailos, P. Sanderson, A. V. Zaragoza, S. McCord, K. Armstrong and P. Styring, *Methanol Worked Examples for the TEA and LCA Guidelines for CO2 Utilization*, 2018.
33 C. Hank, S. Gelpke, A. Schnabl, R. J. White, J. Full, N. Wiebe, T. Smolinka, A. Schaadt, H. M. Henning and C. Hebling, *Sustainable Energy Fuels*, 2018, **2**, 1244.
34 D. Abad, F. Vega, B. Navarrete, A. Delgado and E. Nieto, *Int. J. Hydrogen Energy*, 2021, **46**, 34128–34147.

35 M. Nizami, Slamet and W. W. Purwanto, *J. CO2 Util.*, 2022, **65**, 102253.
36 S. S. Ravi, J. Mazumder, J. Sun, C. Brace and J. W. Turner, *Energy Convers. Manage.*, 2023, **291**, 117271.
37 D. Bellotti, M. Rivarolo, L. Magistri and A. F. Massardo, *J. CO2 Util.*, 2017, **21**, 132–138.
38 K. Atsonios, K. D. Panopoulos and E. Kakaras, *Int. J. Hydrogen Energy*, 2016, **41**, 2202–2214.
39 M. J. Palys and P. Daoutidis, *Comput. Chem. Eng.*, 2022, **165**, 107948.
40 M. J. Bos, S. R. A. Kersten and D. W. F. Brilman, *Appl. Energy*, 2020, **264**, 114672.
41 T. Svitnič and K. Sundmacher, *Appl. Energy*, 2022, **326**, 120017.
42 M. Fasihi, R. Weiss, J. Savolainen and C. Breyer, *Appl. Energy*, 2021, **294**, 116170.
43 R. Nayak-Luke, R. Bañares-Alcántara and I. Wilkinson, *Ind. Eng. Chem. Res.*, 2018, **57**, 14607–14616.
44 EUTurbines, The gas turbine industry's commitments to drive the transition to renewable-gas power generation, **https://www.euturbines.eu/power-the-eu/gas-turbines-renewable-gas-ready/commitments/**, accessed 15 October 2019.
45 D. D. Papadias and R. K. Ahluwalia, *Int. J. Hydrogen Energy*, 2021, **46**, 34527–34541.
46 J. Andersson and S. Grönkvist, *Int. J. Hydrogen Energy*, 2019, **44**, 11901–11919.
47 M. Fasihi, O. Efimova and C. Breyer, *J. Clean Prod.*, 2019, **224**, 957–980.
48 U.S. DOE Hydrogen and Fuel Cells Program, *System Level Analysis of Hydrogen Storage Options*, Washington, D.C., 2019.
49 Matlab, Statistics and Machine Learning Toolbox, **https://se.mathworks.com/products/statistics.html**, accessed 25 December 2022.
50 W. Short, D. Packey and T. Holt, *A manual for the economic evaluation of energy efficiency and renewable energy technologies*, National Renewable Energy Laboratory (NREL), Golden, NREL/TP-462-5173, 1995.
51 Mosek, MOSEK Optimization Toolbox for MATLAB 9.3.22, **https://www.mosek.com/documentation/**, accessed 18 March 2021.
52 A. Aghahosseini and C. Breyer, *Energy Convers. Manage.*, 2018, **169**, 161–173.
53 A.-K. Gerlach, D. Stetter, J. Schmid and C. Breyer, *30th ISES Biennial Solar World Congress, Aug 28 - Sep 2*, Kassel, 2011, vol. 2, pp. 1972–1978.
54 T. Huld, M. Šúri and E. D. Dunlop, *Prog. Photovoltaics Res. Appl.*, 2008, **16**, 595–607.
55 S. Afanasyeva, D. Bogdanov and C. Breyer, *Sol. Energy*, 2018, **173**, 173–191.
56 D. Bogdanov and C. Breyer, *Energy Convers. Manage.*, 2016, **112**, 176–190.
57 M. Decker, F. Schorn, R. C. Samsun, R. Peters and D. Stolten, *Appl. Energy*, 2019, **250**, 1099–1109.
58 C. Chen and A. Yang, *Energy Convers. Manage.*, 2021, **228**, 113673.
59 Y. Rahmat, S. Maier, F. Moser, M. Raab, C. Hoffmann, J. U. Repke and R. U. Dietrich, *Appl. Energy*, 2023, **351**, 121738.
60 M. Bolinger and G. Bolinger, *IEEE J. Photovolt.*, 2022, **12**, 589–594.
61 P. Denholm, M. Hand, M. Jackson and S. Ong, *Land Use Requirements of Modern Wind Power Plants in the United States*, 2009, vol. Technical.
62 M. Fasihi and C. Breyer, *J. Clean Prod.*, 2020, **243**, 118466.
63 Inc. CF Industries Holdings, *Credit Suisse Basic Materials Conference*, 2015.
64 IEA, *IEA G20 hydrogen report: Assumptions*, 2019.
65 Intratec, Methanol Price History & Forecast, **https://www.intratec.us/chemical-markets/methanol-price**, accessed 24 July 2023.
66 Trading Economics, EU Natural Gas, 2023.
67 S. M. W. Wilson, *iScience*, 2022, **25**, 105564.
68 J. F. Wiegner, A. Grimm, L. Weimann and M. Gazzani, *Ind. Eng. Chem. Res.*, 2022, **61**, 12649–12667.
69 M. Sendi, M. Bui, N. Mac Dowell and P. Fennell, *One Earth*, 2022, **5**, 1153–1164.